

# Electron tunneling through proteins

Harry B. Gray\* and Jay R. Winkler\*

Beckman Institute, California Institute of Technology, 1200 E. California Boulevard, Pasadena,  
CA 91125-7400, USA

---

**Abstract.** Electron transfer processes are vital elements of energy transduction pathways in living cells. More than a half century of research has produced a remarkably detailed understanding of the factors that regulate these 'currents of life'. We review investigations of Ru-modified proteins that have delineated the distance- and driving-force dependences of intra-protein electron-transfer rates. We also discuss electron transfer across protein–protein interfaces that has been probed both in solution and in structurally characterized crystals. It is now clear that electrons tunnel between sites in biological redox chains, and that protein structures tune thermodynamic properties and electronic coupling interactions to facilitate these reactions. Our work has produced an experimentally validated timetable for electron tunneling across specified distances in proteins. Many electron tunneling rates in cytochrome *c* oxidase and photosynthetic reaction centers agree well with timetable predictions, indicating that the natural reactions are highly optimized, both in terms of thermodynamics and electronic coupling. The rates of some reactions, however, significantly exceed timetable predictions; it is likely that multistep tunneling is responsible for these anomalously rapid charge transfer events.

## 1. History 342

## 2. Activation barriers 343

- 2.1 Redox potentials 344
- 2.2 Reorganization energy 344

## 3. Electronic coupling 345

## 4. Ru-modified proteins 348

- 4.1 Reorganization energy 349
  - 4.1.1 Cyt *c* 349
  - 4.1.2 Azurin 350
- 4.2 Tunneling timetables 352

## 5. Multistep tunneling 357

## 6. Protein–protein reactions 359

- 6.1 Hemoglobin (Hb) hybrids 359
- 6.2 Cyt *c*/cyt *b*<sub>5</sub> complexes 360
- 6.3 Cyt *c*/cyt *c* peroxidase complexes 360
- 6.4 Zn–cyt *c*/Fe–cyt *c* crystals 361

\* Correspondence may be addressed to either author.

J. R. Winkler: Tel.: 626-395-2834; Fax: 626-449-4159; E-mail: winklerj@caltech.edu

H. B. Gray: Tel.: 626-395-6500; Fax: 626-449-4159; E-mail: hbgray@caltech.edu

**7. Photosynthesis and respiration 362**

7.1 Photosynthetic reaction centers (PRCs) 362

7.2 Cyt c oxidase (CcO) 364

**8. Concluding remarks 365****9. Acknowledgments 366****10. References 366****1. History**

Electron-transfer (ET) reactions are essential components of the energy transduction pathways in living cells. Albert Szent-Györgyi noted in 1941 that ‘in part of the oxidation system electrons wander directly from enzyme to enzyme’ (Szent-Györgyi, 1941). A paradox arose from this observation because it was known that respiratory enzymes are immobilized in membranes. Although two enzymes could be arranged so that redox cofactors could be placed in close proximity for ET, ‘it is geometrically impossible to so arrange a whole series’ (Szent-Györgyi, 1941). Szent-Györgyi proposed that electrons traveled between enzymes in energy bands analogous to those found in semi-conductors. In 1949, however, Evans and Gergely pointed out that the energy gap between filled and empty bands in a polypeptide structure is much larger than  $k_B T$ , seemingly eliminating thermal semi-conductivity as the mechanism of biological electron flow through proteins (Evans & Gergely, 1949).

As the components and reactions of respiration and oxidative phosphorylation became better defined, the electron flow that accompanied this process became more puzzling. In 1956 Chance and Williams struggled to explain electron transport along the respiratory chain (Chance & Williams, 1956). A rigid structure with immobilized redox centers, they argued, would require that the encapsulating polypeptides act as electron conductors or semi-conductors. However, it was difficult to reconcile such a model with many properties of the enzymes. Instead, they suggested that thermally promoted conformational changes could bring redox cofactors into contact and facilitate electron transport along a chain. The reaction probability would depend on the conformational states of adjacent molecules and the overall kinetics of electron flow would be regulated by the dynamics of conformational changes.

A possible resolution to the biological electron flow problem was suggested a decade later by the experiments of DeVault and Chance (De Vault & Chance, 1966; De Vault *et al.* 1967). They found that the rate of cytochrome oxidation in *Chromatium vinosum* reaction centers decreased from  $\sim 3 \times 10^5 \text{ s}^{-1}$  at room temperature to  $\sim 3 \times 10^2 \text{ s}^{-1}$  at 100 K and lower temperatures. The temperature independence indicated that the electron was tunneling between redox sites. In 1974, Hopfield described a thermally activated tunneling model that described the ET kinetics (Hopfield, 1974). Moreover, Hopfield predicted that ET rates between proteins would decrease exponentially as the separation between redox centers increased; his calculated distance-decay constant ( $\beta$ ) was  $1.44 \text{ \AA}^{-1}$ . The structure of the bacterial reaction center was not known at the time, but Hopfield’s model allowed him to estimate an  $8\text{-}\text{\AA}$  edge-to-edge distance between the ET partners.

Our observation in early 1982 of rapid  $18\text{-}\text{\AA}$  ET from Ru(II) to Fe(III) in  $\text{Ru}(\text{NH}_3)_5(\text{His33})\text{-Fe-cytochrome } c$  (cyt *c*) demonstrated that long-range electron tunneling is a viable mechanism for biological electron flow (Winkler *et al.* 1982). Following this discovery, there was

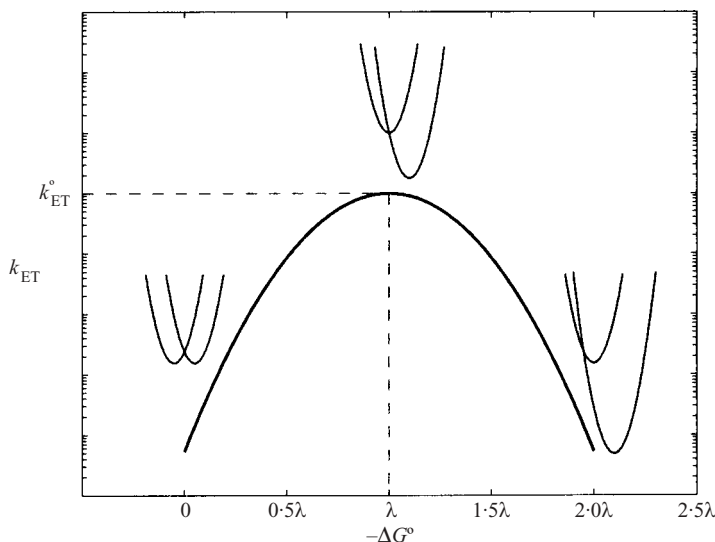


**Fig. 1.** Driving-force dependence of ET rates predicted by semi-classical theory [Eq. (1)]. Rates increase with driving force until they reach a maximum value ( $k_{ET}^{\circ}$ ) at  $-\Delta G^{\circ} = \lambda$ . Rates then decrease at higher driving forces (inverted effect).

an explosion of research on electron tunneling kinetics in model systems and in proteins (Pasman *et al.* 1982; Calcaterra *et al.* 1983; Freed, 1983; McGourty *et al.* 1983; Overfield *et al.* 1983; Simolo *et al.* 1984; Gunner *et al.* 1986; Heitele *et al.* 1987; Kuki & Wolynes, 1987; Closs & Miller, 1988; Lawson *et al.* 1989; Moser *et al.* 1992; Wasielewski, 1992; Evenson & Karplus, 1993; Gray & Winkler, 1996; Kuznetsov & Ulstrup, 1998; Skourtis & Beratan, 1998; Verhoeven, 1999; Winkler, 2000; Gray & Winkler, 2001, 2003; Paddon-Row, 2003). It is now clear that electrons tunnel between sites in biological redox chains, and that protein structures tune thermodynamic properties and electronic coupling interactions to facilitate these reactions.

## 2. Activation barriers

According to classical (Marcus) theory, the activation barrier for an adiabatic ET reaction depends on two parameters, the driving force ( $-\Delta G^{\circ}$ ) and the reorganization energy ( $\lambda$ ) (Marcus & Sutin, 1985). The reorganization parameter ( $\lambda$ ) reflects the extent of outer-sphere ( $\lambda_{out}$ ) and inner sphere ( $\lambda_{in}$ ) nuclear rearrangement that accompanies charge transfer. The  $\lambda$ -values for a cross reaction can be estimated from the self-exchange reorganization energies for each redox partner (i.e.  $\lambda_{12} \approx \frac{1}{2}\lambda_{11} + \frac{1}{2}\lambda_{22}$ ).

The central lesson of classical theory is that nuclear rearrangements accompanying ET must be compensated for by reaction driving force (Fig. 1). The balance between  $\Delta G^{\circ}$  and  $\lambda$  is a direct consequence of protein structure. A Landau–Zener treatment of the reactant–product transition probability produces the familiar semi-classical expression for the rate of non-adiabatic ET between a donor (D) and acceptor (A) held at fixed distance [Eq. (1)] (Marcus & Sutin, 1985):

$$k_{ET} = \sqrt{\frac{4\pi^3}{\hbar^2 \lambda RT}} H_{AB}^2 \exp \left\{ -\frac{(\Delta G^{\circ} + \lambda)^2}{4\lambda RT} \right\}, \quad (1)$$

Biological electron flow over long distances with a relatively small release of free energy is possible because the protein fold creates a suitable balance between  $\Delta G^\circ$  and  $\lambda$  as well as adequate electronic coupling between distant redox centers.

## 2.1 Redox potentials

The reduction potentials of redox-active proteins are exquisitely sensitive to the structure of the polypeptide (Battistuzzi *et al.* 1997, 2001; Gray *et al.* 2000; Springs *et al.* 2002). It is well known that homologous proteins from different organisms can have quite disparate amino-acid sequences yet nearly identical three-dimensional (3D) structures (Moore & Pettigrew, 1990; Scott & Mauk, 1996). Nevertheless, single-point mutations can destroy redox function without disrupting structure. Indeed, substitution of a single amino acid in myoglobin (Mb) can shift the Fe(III/II) reduction potential by as much as 200 mV, effecting a greater than 1000-fold change in the equilibrium constant for reaction with a redox partner (Varadarajan *et al.* 1989).

The secondary and tertiary structures of a protein can modulate the reduction potential of a single cofactor by more than 500 mV. The Fe(III/II) reduction potential of a free heme in aqueous solution is approximately  $-200$  mV *versus* NHE, the potential of cyt *c* is 260 mV, and that of cyt *f* reaches 450 mV (Tezcan *et al.* 1998; Battistuzzi *et al.* 2002). The shift in reduction potential is reflected in a differential folding free energy of the oxidized and reduced proteins (Churg & Warshel, 1986; Bixler *et al.* 1992; Pascher *et al.* 1996; Winkler *et al.* 1997). In the case of cyt *f*, the Fe(II) protein is more stable toward unfolding than the oxidized protein (Sabahi & Wittung-Stafshede, 2002); the redox potential indicates a stability differential of some 650 meV ( $63 \text{ kJ mol}^{-1}$ ). In order for cyt *f* to be a viable redox protein, the folding free energy of the oxidized form must be at least  $2 k_B T$  ( $\sim 5 \text{ kJ mol}^{-1}$  at 298 K), requiring that the folding free energy of the reduced protein be greater than  $68 \text{ kJ mol}^{-1}$  (700 meV).

## 2.2 Reorganization energy

The protein fold plays a central role in lowering the reorganization energy of a biological ET reaction (Winkler *et al.* 1997; Gray *et al.* 2000). A large part of the  $\lambda$ -reduction results from sequestering a redox center from the aqueous solvent environment. Continuum models suggest that embedding a redox center inside a low dielectric cavity can lower the outer-sphere reorganization energy by as much as 50% (Simonson, 2002). Moreover, by constraining the coordination environment around metal centers, inner-sphere reorganization energy can also be reduced (Gray *et al.* 2000). Indeed, metals that are typically poor redox reagents because of large reorganization barriers can be extremely efficient when embedded in protein interiors. Copper is a case in point. The reorganization energy for electron self-exchange in  $\text{Cu}(\text{phen})_2^{2+/+}$  is  $\sim 2.4$  eV; the value for Cu(II/I) in *Pseudomonas aeruginosa* azurin is 0.7 eV (see below). The 1.7-eV reduction in  $\lambda$  reflects the transition-state stabilization imposed by the azurin fold (Winkler *et al.* 1997).

Two approaches are commonly employed to estimate reorganization energies in ET reactions: the first involves driving-force variations; and the second is based on temperature dependences. Carefully designed studies of the variation of rates with driving force can lead to reliable estimates of  $\lambda$  (McLendon & Miller, 1985; Closs & Miller, 1988; Meade *et al.* 1989; Fox *et al.* 1990; McCleskey *et al.* 1992; Mines *et al.* 1996), but there are several pitfalls. To begin with, it can be difficult to modify natural redox sites sufficiently to define  $\lambda$  with confidence. At low driving

forces,  $\ln(k_{\text{ET}})$  varies linearly with  $-\Delta G^\circ$ , and the slope is independent of  $\lambda$ . Reorganization energies extracted from these data are fraught with uncertainty because they involve the analysis of small deviations from linearity. In principle, more reliable values of  $\lambda$  can come from measurements at driving forces close to the reorganization energy, where rates reach a maximum and the driving-force curve flattens. Complications can arise, however, in redox processes where ET is not rate limiting. Conformationally gated reactions are a prime example of this type of behavior (Hoffman & Ratner, 1987; Brunschwig & Sutin, 1989).

Reorganization energies also can be extracted from studies of the temperature dependence of ET rates (Skov *et al.* 1998). These would seem to be more direct and reliable than driving-force studies. The drawback, however, is that accurate  $\lambda$ -values can be extracted only when the temperature dependence of  $\Delta G^\circ$  has been determined as well (Marcus & Sutin, 1975). In many cases, particularly with deeply buried redox sites, reduction potentials are not known with great accuracy and temperature dependences are beyond available measurement methods.

Finally, it is important to remember that the reorganization energy is a composite parameter rather than a fundamental physical quantity. Refinements to the semi-classical theory usually arise from quantum mechanical treatments of vibrational motions (Brunschwig & Sutin, 1987). The increased rigor associated with these models, however, is rarely accompanied by the extra data required to cope with the influx of new parameters. The approximations involved in its definition, and the errors associated with its measurement dictate that  $\lambda$  should never be expressed with great precision. At the present level of experiment and theory, it is difficult to justify uncertainties in  $\lambda$  of less than 100 meV.

### 3. Electronic coupling

The ability to control redox potentials and reorganization energies in proteins comes at a price: ET partners buried within insulating polypeptides cannot come into close contact. Reactions are, therefore, non-adiabatic and the essential electronic interaction between redox cofactors must be mediated by the polypeptide matrix. Our extensive experimental investigations of the distance dependences of ET rates have been aimed at elucidating the fundamental principles of distant electronic couplings between redox sites in Ru-modified proteins (Winkler & Gray, 1992; Gray & Winkler, 1996; Winkler *et al.* 1999). Distance dependences initially were investigated by labeling alternate His residues on proteins from different organisms. The development of routine site-directed mutagenesis techniques permitted the placement of His residues at many different surface sites in a single protein.

The electronic coupling matrix element ( $H_{\text{AB}}$ ) reflects the strength of the interaction between reactants and products at the nuclear configuration of the transition state. Hopfield's square-barrier tunneling model predicts that the coupling will depend exponentially on the distance ( $r$ ) between redox centers [Eq. (2)] (Hopfield, 1974):

$$H_{\text{AB}}(r) = H_{\text{AB}}(r_0) \exp\left\{-\frac{1}{2}\beta(r-r_0)\right\}. \quad (2)$$

A square tunneling barrier implies that a homogeneous medium separates the donor and acceptor. This model is appropriate for electron tunneling across a vacuum ( $\beta = 3\text{--}5 \text{ \AA}^{-1}$ ) and is a reasonable approximation for tunneling through glassy solvents [ $\text{H}_2\text{O}$ ,  $\beta = 1.65 \text{ \AA}^{-1}$  (Ponce *et al.* 2000); 2-methyltetrahydrofuran,  $\beta = 1.2 \text{ \AA}^{-1}$  (Miller *et al.* 1984)]. Superexchange models are better suited to the description of tunneling through inhomogeneous media. In 1961,

McConnell described a superexchange model for electron tunneling from a donor to an acceptor across a bridge composed of  $n$  identical repeat units (McConnell, 1961). The electronic coupling matrix element proves to be a function of the individual couplings between redox sites and the bridge ( $b_{Ab}$ ,  $b_{bB}$ ), the coupling between bridge elements ( $b_{bb}$ ), and the gap ( $\Delta\epsilon$ ) between the energy of tunneling electron (hole) and reduced (oxidized) bridge states [Eq. (3)].

$$H_{AB} = \frac{b_{Ab}}{\Delta\epsilon} \left( \frac{b_{bb}}{\Delta\epsilon} \right)^{n-1} b_{bB}. \quad (3)$$

The medium separating redox sites in proteins is comprised of a complex array of bonded and non-bonded contacts and an *ab initio* calculation of coupling strengths is a formidable challenge (Stuchebrukhov, 2001). The homologous-bridge superexchange model [Eq. (3)] is not suitable because of the diverse interactions in proteins. Beratan, Onuchic, and co-workers developed a generalization of the McConnell superexchange coupling model that accommodates the structural complexity of a protein matrix (Beratan *et al.* 1987, 1991, 1992; Beratan & Onuchic, 1989; Onuchic & Beratan, 1990; Onuchic *et al.* 1992). In this tunneling-pathway model, the medium between D and A is decomposed into smaller subunits linked by covalent bonds, hydrogen bonds, or through-space jumps. Each link is assigned a coupling decay ( $\epsilon_C$ ,  $\epsilon_H$ ,  $\epsilon_S$ ), and a structure-dependent searching algorithm is used to identify the optimum coupling pathway between the two redox sites. The total coupling of a single pathway is given as a repeated product of the couplings for the individual links [Eq. (4)]:

$$H_{AB} \propto \prod \epsilon_C \prod \epsilon_H \prod \epsilon_S. \quad (4)$$

A tunneling pathway can be described in terms of an effective covalent tunneling path comprised of  $n$  (non-integral) covalent bonds, with a total length equal to  $\sigma_I$  [Eq. (5a, b)].

$$H_{AB} \propto (\epsilon_C)^n, \quad (5a)$$

$$\sigma_I = n \times 1.4 \text{ \AA/bond}. \quad (5b)$$

The relationship between  $\sigma_I$  and the direct D–A distance ( $r$ ) reflects the coupling efficiency of a pathway (Langen *et al.* 1995). The variation of ET rates with  $r$  depends upon the coupling decay for a single covalent bond ( $\epsilon_C$ ). Equation (3) suggests that the magnitude of  $\epsilon_C$  should depend critically upon the energy of the tunneling electron relative to the energies of the bridge hole and electron states (Regan *et al.* 1995). Clear demonstrations of this energy dependence in the tunneling regime have been elusive. Studies, however, have shown that electron transport over exceptionally long distances is possible when hole or electron states of the bridge can be populated as real intermediates (Jortner *et al.* 1998; Davis *et al.* 2002). In comparing ET data from different protein systems, then, it is important to consider the tunneling-energy gap and the possibility of forming oxidized or reduced intermediates in the bridging medium.

The tunneling-pathway model has proved to be one of the most useful methods for estimating distant electronic couplings (Beratan *et al.* 1987; Onuchic & Beratan, 1990; Onuchic *et al.* 1992). Employing this model, Beratan, Betts, and Onuchic predicted in 1991 that proteins comprised largely of  $\beta$ -sheet structures would be more effective at mediating long-range couplings than those built from  $\alpha$ -helices (Beratan *et al.* 1991). This analysis can be taken a step further by comparing the coupling efficiencies of individual protein secondary structural elements ( $\beta$ -sheets,  $\alpha$ -helices). The coupling efficiency can be determined from the variation of  $\sigma_I$  as a function of  $r$ .

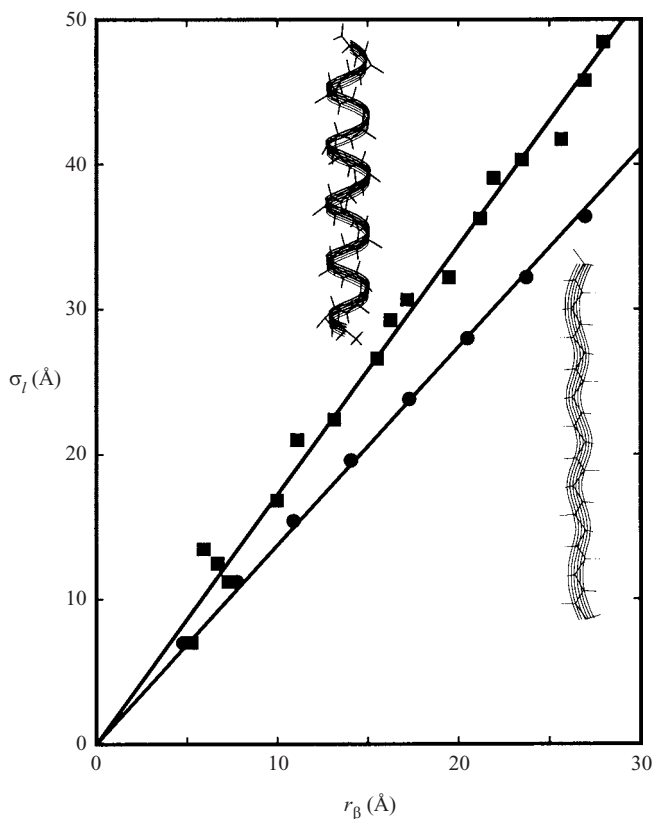


**Fig. 2.** Relationship between tunneling path length ( $\sigma_l$ ) and  $\beta$ -carbon separation predicted by tunneling pathway analysis of idealized  $\alpha$ -helices (■) and  $\beta$ -strands (●). The steeper slope for the  $\alpha$ -helical structure suggests that it is a less efficient tunneling medium.

A linear  $\sigma_l/r$  relationship implies that  $k_{ET}^o$  will be an exponential function of  $r$ ; the distance-decay constant is determined by the slope of the  $\sigma_l/r$  plot and the value of  $\epsilon_C$ .

A  $\beta$ -sheet is comprised of extended polypeptide chains interconnected by hydrogen bonds; the individual strands of  $\beta$ -sheets define nearly linear coupling pathways along the peptide backbone spanning  $3.4 \text{ \AA}$  per residue. The tunneling length for a  $\beta$ -strand exhibits an excellent linear correlation with  $\beta$ -carbon separation ( $r_\beta$ , Fig. 2); the best linear fit with zero intercept yields a slope of  $1.37 \sigma_l/r_\beta$  (distance-decay constant  $= 1.0 \text{ \AA}^{-1}$ ). Couplings across a  $\beta$ -sheet depend upon the ability of hydrogen bonds to mediate the D/A interaction. The standard parameterization of the tunneling-pathway model defines the coupling decay across a hydrogen bond in terms of the heteroatom separation [Eq. (6)]:

$$\epsilon_H = \epsilon_C^2 \exp[-1.7(r - 2.8)]. \quad (6)$$

If the two heteroatoms are separated by twice the  $1.4\text{-\AA}$  covalent-bond distance, then the hydrogen-bond decay is assigned a value equal to that of a covalent bond (Onuchic *et al.* 1992). Longer heteroatom separations lead to weaker predicted couplings but, as yet, there is no experimental confirmation of this relationship.

In the coiled  $\alpha$ -helix structure a linear distance of just  $1.5 \text{ \AA}$  is spanned per residue. In the absence of mediation by hydrogen bonds,  $\sigma_l$  is a very steep function of  $r_\beta$ , implying that



an  $\alpha$ -helix is a poor conductor of electronic coupling ( $2.7 \sigma_{\parallel}/r_{\beta}$ , distance-decay constant =  $1.97 \text{ \AA}^{-1}$ ) (Langen *et al.* 1995). If the hydrogen-bond networks in  $\alpha$ -helices mediate coupling, then the Beratan–Onuchic parameterization of hydrogen-bond couplings suggests a  $\sigma_{\parallel}/r_{\beta}$  ratio of 1.72 (distance-decay constant =  $1.26 \text{ \AA}^{-1}$ , Fig. 2). Treating hydrogen bonds as covalent bonds further reduces this ratio ( $1.29 \sigma_{\parallel}/r_{\beta}$ , distance-decay constant =  $0.94 \text{ \AA}^{-1}$ ). Hydrogen-bond interactions, then, will determine whether  $\alpha$ -helices are vastly inferior to or are slightly better than  $\beta$ -sheets in mediating long-range electronic couplings. It is important to note that the coiled helical structure leads to poorer  $\sigma_{\parallel}/r_{\beta}$  correlations, especially for values of  $r_{\beta}$  under  $10 \text{ \AA}$ . In this distance region, the tunneling-pathway model predicts little variation in coupling efficiencies for the different secondary structures (Fig. 2). The coupling in helical structures could be highly anisotropic. ET along a helix may have a very different distance dependence from ET across helices. In the latter cases, the coupling efficiency will depend on the nature of the interactions between helices. A final point involves the dependence of coupling efficiencies on bond angles. It is well known that  $\beta$ -sheets and  $\alpha$ -helices are described by quite different peptide bond angles ( $\phi, \psi$ ). *Ab initio* calculations on saturated hydrocarbons have suggested that different conformations produce different couplings (Liang & Newton, 1992). Different values of  $\epsilon_C$ , then, might be necessary to describe couplings in  $\beta$ -sheets and  $\alpha$ -helices.

The original tunneling-pathway model successfully described the distance dependence of protein ET reactions when a single pathway dominated the coupling (Onuchic *et al.* 1992). The model was less successful when multiple pathways contributed to the overall coupling. More elaborate computational protocols have since been developed to describe in greater detail the factors that determine distant couplings in proteins (Stuchebrukhov, 1996; Skourtis & Beratan, 1997; Balabin & Onuchic, 1998; Kumar *et al.* 1998; Regan & Onuchic, 1999).

Analyses of ET rate/distance relationships require a consistent definition of the D–A distance. When comparing rates from systems with different donors and/or acceptors, it can be difficult to identify a proper distance measure. All maximum ET rates should extrapolate to a common adiabatic rate as  $r$  approaches van der Waals contact. So-called edge-to-edge distances are often employed but there are many ambiguities, not the least of which is defining the set of atoms that constitute the edges of D and A. For planar  $\pi$ -aromatic molecules (e.g. chlorophylls, pheophytins, quinones), edge–edge separations are usually defined on the basis of the shortest distance between aromatic carbon atoms of D and A. In metal complexes (e.g. Fe–heme, Ru–amine, Ru–bpy), however, atoms on the periphery are not always well coupled to the central metal (Newton, 1988), and empirical evidence suggests that metal–metal distances are more appropriate. This dichotomy is by no means rigorously supported by experimental data but, instead, represents the best available compromise. In the following analyses, edge–edge distances will be used for ET reactions between  $\pi$ -aromatic donors and acceptors, metal–metal separations will be used for reactions involving two transition-metal complexes, and edge–metal distances will be used for mixed (metal/ $\pi$ -aromatic) D–A reactions.

#### 4. Ru-modified proteins

Semi-classical theory provides a framework for understanding biological electron flow; what is necessary on the experimental front are systematic investigations of the response of rates to variations in ET parameters ( $\Delta G^\circ, \lambda, r$ ). Early efforts involving studies of bimolecular ET reactions were frustrated by the effects of diffusion. A simple bimolecular ET reaction can be



broken into a sequence of three steps (Marcus, 1956): diffusional formation of an encounter or precursor complex [Eq. (7)]:



ET from donor to acceptor within the precursor complex [Eq. (8)]:



and dissociation of the successor complex [Eq. (9)]:



The precursor complex is rarely observed in ET reactions, so it is reasonable to employ the steady-state approximation (i.e.  $\partial[DA]/\partial t = 0$ ) to describe its time dependence. Within the limits of this approximation, the observed second-order rate constant for a bimolecular ET reaction is given by Eq. (10):

$$k_{\text{obs}} = \frac{k_{+D}k_{ET}}{k_{-D} + k_{ET}}. \quad (10)$$

Below the diffusion limit (i.e.  $k_{ET} \ll k_{-D}$ ),  $k_{\text{obs}}$  is equal to  $K_{[DA]}k_{ET}$  (where  $K_{[DA]} = k_{+D}/k_{-D}$  is the equilibrium constant for precursor-complex formation). Since the value of  $K_{[DA]}$  is usually not known, it is quite difficult to extract accurate values of  $\lambda$  and  $H_{AB}$  from low-driving-force bimolecular ET rates (Mauk *et al.* 1980). At high driving forces, reaction rates become masked by diffusion (i.e.  $k_{ET} \gg k_{-D}$ ,  $k_{\text{obs}} = k_{+D}$ ), frustrating efforts to observe inverted driving-force behavior (Rehm & Weller, 1970; Creutz & Sutin, 1977).

In order to circumvent these difficulties, one of us (H.B.G.) initiated a research program in the mid-1970s to study the rates of intramolecular ET reactions in metalloproteins that had been surface-labeled with redox-active metal complexes. The first Ru-modified protein to be prepared and characterized was  $\text{Ru}(\text{NH}_3)_5(\text{His33})\text{-Fe-cyt } c$  (Yocom *et al.* 1982); the rate of ET from Ru(II) to Fe(III) ( $k_{ET} = 30 \text{ s}^{-1}$ ,  $-\Delta G^\circ = 210 \text{ meV}$ ) was measured using photochemical triggering techniques (Winkler *et al.* 1982).

## 4.1 Reorganization energy

### 4.1.1 Cyt c

Our investigations of intramolecular ET in heme proteins have focused mainly on cyt *c* (104 amino acids in the horse protein; 12.5 kDa;  $E^\circ = 0.28 \text{ V}$  versus NHE) (Fig. 3) (Moore & Pettigrew, 1990; Scott & Mauk, 1996). Early work with the Ru–ammine modified protein involved the replacement of the native Fe center with Zn. Long-range ET reactions were initiated by visible-light excitation of the resulting Zn–porphyrin (ZnPor) to its long-lived ( $> 10 \text{ ms}$ ), strongly reducing ( $E^\circ \sim -0.8 \text{ V}$  versus NHE) triplet excited state (Elias *et al.* 1988). A driving-force study of ET rates in  $\text{Ru}(\text{NH}_3)_4\text{L}(\text{His33})$ -modified Zn-substituted cyt *c* (L =  $\text{NH}_3$ , pyridine, isonicotinamide) was consistent with  $\lambda_{12} = 1.2 \text{ eV}$  (Meade *et al.* 1989). The self-exchange reorganization energies for Ru–ammine complexes ( $\lambda_{11}$ ) are in the vicinity of 1.6 eV (Brown & Sutin, 1979; Marcus & Sutin, 1985). Intramolecular ET kinetics, then, suggest that  $\lambda_{22} = 0.8 \text{ eV}$  for Zn–cyt *c*.



**Fig. 3.** Ribbon representation of the peptide backbone in horse-heart cyt *c*. The heme and its axial ligands are shown in black.

Studies of high-driving-force ET in heme and non-heme proteins were made possible by Ru–diimine labeling protocols and the ‘flash-quench’ triggering method (Fig. 4) (Chang *et al.* 1991a). The driving-force dependence of ET in Ru(diimine)<sub>2</sub>(im)(His33)-modified Fe–cyt *c* is best described by  $\lambda_{12} = 0.8$  eV (Bjerrum *et al.* 1995; Mines *et al.* 1996). This value is lower than that found for Ru–amine-modified Zn–cyt *c* because the diimine ligands coordinated to the Ru center are larger and more hydrophobic than amines. Consequently, the self-exchange reorganization energy for Ru(diimine)<sub>2</sub>(im)(His)<sup>3+/2+</sup> is substantially smaller ( $\lambda_{11} = 0.8$  eV) than that of the ammine (Marcus & Sutin, 1985; Winkler & Gray, 1992). The combined results from ET measurements in the Ru–amine and Ru–diimine proteins suggest that the reorganization energy for electron exchange between Fe(II)–cyt *c* and Fe(III)–cyt *c* is 0.8(1) eV.

#### 4.1.2 Azurin

The flash-quench method made it possible for us to examine high-driving-force ET in labeled copper proteins. *P. aeruginosa* azurin (Fig. 5) has a Cu(II/I) reduction potential of 0.31 V *versus* NHE (Adman & Jensen, 1981; Chang *et al.* 1991b; Pascher *et al.* 1993). Analysis of the driving-force dependence of Cu(I) → M(III) (M = Ru, Os) ET in M(diimine)<sub>2</sub>(im)(His83)–azurin

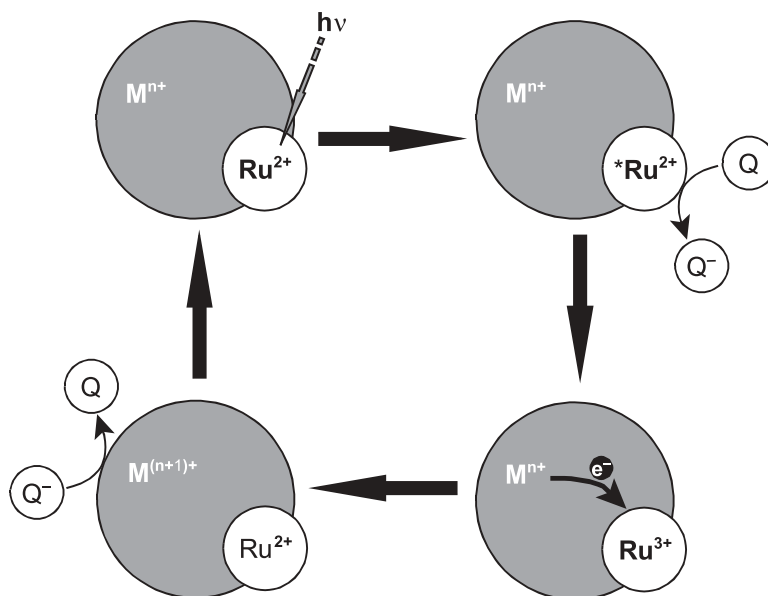


**Fig. 4.** The *intermolecular* flash-quench scheme for measuring ET rates. The photosensitizer ( $\text{Ru}^{2+}$ ) is excited by a short laser pulse. A quencher in solution oxidizes the excited sensitizer. In a subsequent *intramolecular* reaction, the protein metal center transfers an electron to the oxidized sensitizer ( $\text{Ru}^{3+}$ ). In a much slower step, the reduced quencher transfers an electron to the oxidized protein metal center to regenerate the original species.

gives a reorganization energy of 0.8 eV (Di Bilio *et al.* 1997). In accord with this finding, the temperature independence (240–300 K) of  $\text{Cu(I)} \rightarrow \text{Ru(III)}$  ET in  $\text{Ru(bpy)}_2(\text{im})(\text{His83})$ –azurin can be described by  $\lambda_{12} = 0.7 \pm 0.1$  eV, although the observed twofold increase in rate constant as the temperature is lowered to 170 K cannot be explained by changes in the exponential term of the semi-classical rate expression (Skov *et al.* 1998). It is more likely that the Ru–Cu electronic coupling (see below) increases as the protein is cooled to 170 K.

Rates of Ru(III) and Os(III) reduction by Cu(I) have been measured in single crystals of *P. aeruginosa*  $\text{M}(\text{diimine})_2(\text{im})(\text{His83})$ –azurin; in these cases, protein conformation and surface solvation are precisely defined by high-resolution X-ray structure determinations (Crane *et al.* 2001). The time constants for electron tunneling in crystals are roughly the same as those measured in solution, indicating very similar protein structures in the two states. High-resolution structures of the oxidized (1.5 Å) and reduced (1.4 Å) forms of  $\text{Ru(tpy)(bpy)(im)(His83)}$ –azurin establish that very small changes in copper coordination accompany reduction (Crane *et al.* 2001). Although  $\text{Ru(bpy)}_2(\text{im})(\text{His83})$ –azurin is less solvated in the crystal lattice, the reorganization energy for  $\text{Cu(I)} \rightarrow \text{Ru(III)}$  ET falls in the same range (0.6–0.8 eV) determined experimentally for the reaction in solution. It is striking that driving forces, reorganization energies, and rates of  $\text{Cu(I)} \rightarrow \text{M(III)}$  ( $\text{M} = \text{Ru, Os}$ ) ET are virtually unchanged when labeled azurins lose one-third of their solvent-accessible surface upon transfer from dilute solutions to crystal lattices with just 40% water. These observations suggest that bulk water plays a minor role in azurin ET reactions; what little solvent reorganization occurs is likely to involve only the ordered waters of hydration.



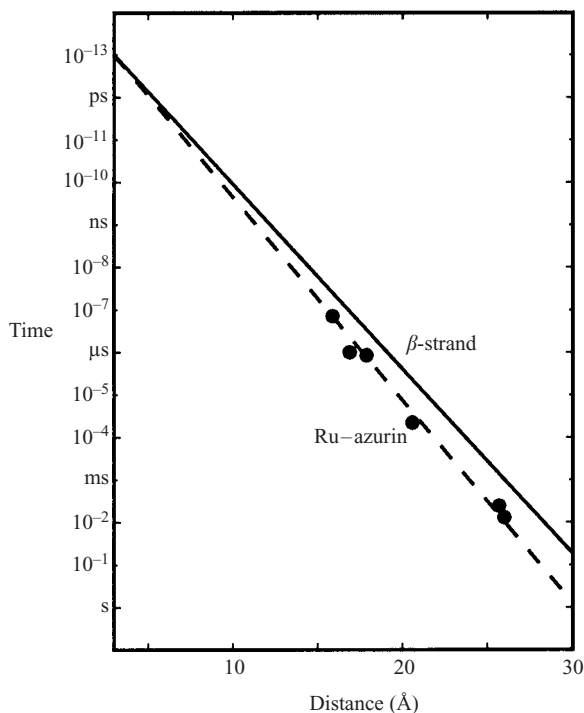
**Fig. 5.** Ribbon representation of the peptide backbone in *Pseudomonas aeruginosa* azurin. The Cu cofactor and its ligands are shown in black.

#### 4.2 Tunneling timetables

Theoretical analyses of coupling pathways in proteins suggest that the efficiency of distant electron tunneling depends on the secondary structure of the polypeptide between the redox centers (Beratan *et al.* 1991). To determine the efficiency of coupling across  $\beta$ -sheet structures, we examined distance dependences of ET in azurin (Langen *et al.* 1995; Regan *et al.* 1995). The copper center in azurin is situated at one end of an 8-stranded  $\beta$ -barrel, ligated in a trigonal plane by two imidazoles (His46, His117) and a thiolate (Cys112); in addition, there are weak axial interactions (Met121 thioether sulfur, Gly45 carbonyl oxygen) (Adman & Jensen, 1981; Adman, 1991). The azurin from *P. aeruginosa* has two additional His residues, one of which (His83) reacts readily with Ru-labeling reagents. A H83Q base mutant was prepared and individual mutant His residues were introduced at five locations on  $\beta$ -strands extending from the Cys112 and

**Table 1.** Driving-force-optimized intramolecular ET rates and Ru–Cu distances in *Ru(bpy)<sub>2</sub>(im)(His)<sup>2+</sup>-modified azurin*

Modified His <sup>a</sup>	$k_{\text{ET}}^{\circ}$ (s <sup>-1</sup> )	<i>R</i> (Å)
83	$1.0(1) \times 10^6$	16.9
107	$2.4(5) \times 10^2$	25.7
109	$8.5(10) \times 10^5$	17.9
122	$7.1(4) \times 10^6$	15.9
124	$2.2(2) \times 10^4$	20.6
126	$1.3(6) \times 10^2$	26.0

<sup>a</sup>References: Langen (1995); Langen *et al.* (1995); Regan *et al.* (1995).**Fig. 6.** Distance dependence of driving-force-optimized ET rates in Ru-labeled *P. aeruginosa* azurin. The solid line is the distance decay predicted by the tunneling pathway model for ET along an ideal  $\beta$ -strand ( $\beta = 1.0 \text{ \AA}^{-1}$ ). The dashed line is the best fit to the data ( $\beta = 1.1 \text{ \AA}^{-1}$ ).

Met121 ligands (K122H, T124H, T126H, Q107H, M109H). Measurements of  $\text{Cu(I)} \rightarrow \text{Ru(bpy)}_2\text{-(im)(HisX)}^{3+}$  ET ( $-\Delta G^\circ = 0.7 \text{ eV}$ ) provide a calibration for the distance dependence of ET along  $\beta$ -strands (Table 1, Fig. 6). The driving-force-optimized electron tunneling timetable for azurin reveals a nearly perfect exponential distance dependence, with a decay constant ( $\beta$ ) of  $1.1 \text{ \AA}^{-1}$ , and an intercept at close contact ( $r_0 = 3 \text{ \AA}$ ) of  $10^{13} \text{ s}^{-1}$ . This decay constant is quite similar to that found for superexchange-mediated tunneling across saturated alkane bridges ( $\beta \approx 1.0 \text{ \AA}^{-1}$ ) (Smalley *et al.* 1995, 2003), strongly indicating that a similar coupling mechanism is operative in the polypeptide.

The validity of the azurin tunneling timetable rests on the assumption that Ru–azurin structures are not very different in crystals and aqueous solutions. Our measurements of ET kinetics

**Table 2.** Driving-force-optimized intramolecular ET rates and Ru–Fe distances in *Ru(bpy)<sub>2</sub>(im)(His)<sup>2+</sup>-modified cyt c*

Modified His <sup>a</sup>	$k_{\text{ET}}^{\circ}$ (s <sup>-1</sup> )	<i>R</i> (Å)	Ref.
33 <sup>b</sup>	$2.7 \times 10^6$	17.9	Chang <i>et al.</i> (1991a)
39 <sup>c</sup>	$3.3 \times 10^6$	20.3	Wuttke <i>et al.</i> (1992)
54 <sup>d,e</sup>	$3.4 \times 10^4$	22.5	Karpishin <i>et al.</i> (1994)
54(Ile52) <sup>d,f</sup>	$5.8 \times 10^4$	21.5	Karpishin <i>et al.</i> (1994)
58 <sup>d,g</sup>	$6.0 \times 10^4$	20.2	Casimiro <i>et al.</i> (1993)
62 <sup>d,h</sup>	$1.0 \times 10^4$	20.2	Wuttke <i>et al.</i> (1992)
66 <sup>d,i</sup>	$1.1 \times 10^6$	18.9	Casimiro <i>et al.</i> (1993)
72 <sup>b,j</sup>	$9.4 \times 10^5$	13.8	Wuttke <i>et al.</i> (1992)

<sup>a</sup>The horse-heart numbering system is used for all of the cytochromes *c*; <sup>b</sup>Horse-heart cyt *c*; <sup>c</sup>*Candida krusei* cyt *c*; <sup>d</sup>*Saccharomyces cerevisiae* cyt *c*; <sup>e</sup>Lys54His,Cys102Ala double mutant; <sup>f</sup>Lys54His,Asn52Ile,Cys102Ala triple mutant; <sup>g</sup>Leu58His,His39Gln,Cys102Ser triple mutant; <sup>h</sup>Asn62His mutant; <sup>i</sup>Glu66His,His39Gln,Cys102Ser triple mutant; <sup>j</sup>Lys72His semi-synthetic variant.

**Table 3.** Driving-force-optimized intramolecular ET rates and Ru–Fe distances in *Ru(bpy)<sub>2</sub>(im)(His)<sup>2+</sup>-modified Mb<sup>a</sup>*

Modified His	$k_{\text{ET}}^{\circ}$ (s <sup>-1</sup> )	<i>R</i> (Å)
70	$1.6 \times 10^7$	16.6
83	$2.5 \times 10^3$	18.9
95	$2.3 \times 10^6$	18.0

<sup>a</sup>See Langen *et al.* (1996).

on crystalline samples of labeled azurins directly test this assumption (Crane *et al.* 2001). We find that the rate constants for oxidation of Cu(I) by Ru(III) and Os(III) in solutions and crystals are nearly identical for each donor–acceptor pair (Table 1). It follows that the crystal structures of reduced and oxidized azurin are the relevant reactant and product states for solution ET.

It is important to distinguish between superexchange-mediated electron tunneling and multi-step mechanisms that can also move charge over large molecular distances. In tunneling processes, quantum mechanical mixing of localized donor and acceptor states with oxidized (and/or reduced) bridge states couples the reactant and product states, producing an avoided crossing between the free-energy surfaces at the transition state. Importantly, oxidized (reduced) bridge states are not populated in tunneling reactions; ET occurs in a single elementary reaction step. Because redox centers in metalloenzymes cannot come into close contact, electrons must tunnel between them. There is a practical upper limit to the separation distance between redox sites; if charges must be transferred farther than this range, then multiple tunneling steps are required. Long-range ET can proceed by either mechanism, but each has distinct energetic and coupling requirements, and can respond quite differently to changes in reaction parameters (e.g. *T*,  $\Delta G^{\circ}$ ).

The energy gap between the donor/acceptor redox levels and those of oxidized or reduced intermediate states is the primary criterion in determining when multistep tunneling becomes important (see below). In proteins with a single redox cofactor, the opportunities for multistep tunneling are limited. Extreme redox potentials are necessary to oxidize and reduce polypeptide backbones; thus multistep tunneling via backbone states will not contribute to observed

**Table 4.** Driving-force-optimized intramolecular ET rates and Ru–Fe distances in *Ru(bpy)<sub>2</sub>(im)(His)<sup>2+</sup>-modified cyt b<sub>562</sub>*<sup>a</sup>

Modified His	$k_{ET}^o$ (s <sup>-1</sup> )	<i>R</i> (Å)
12	$2.6 \times 10^7$	14.2
15	$1.9 \times 10^6$	15.0
19	$6.7 \times 10^4$	21.0
63	$7.9 \times 10^6$	17.0
70	$2.3 \times 10^5$	19.5
73	$4.9 \times 10^2$	21.0
86	$2.9 \times 10^2$	25.0
89	$4.4 \times 10^4$	22.5
92	$1.0 \times 10^7$	18.5

<sup>a</sup>See Winkler *et al.* (1999).**Table 5.** Driving-force-optimized intramolecular ET rates and Ru–Fe distances in *Ru(bpy)<sub>2</sub>(im)(His)<sup>2+</sup>-modified C. vinosum HiPIP*<sup>a</sup>

Modified His	$k_{ET}^o$ (s <sup>-1</sup> )	<i>R</i> (Å)
18	$6.0(10) \times 10^7$	12.8
42	$2.7(5) \times 10^8$	12.3
50	$1.8(2) \times 10^6$	13.7
81	$6.1(10) \times 10^8$	12.2

<sup>a</sup>See Babini *et al.* (2000).

ET kinetics under most solution conditions. The side-chains of certain amino acids (e.g. Tyr, Trp) have redox potentials that are more accessible than those of the peptide backbone (Jovanic *et al.* 1986; Harriman, 1987; DeFelippis *et al.* 1989; Stubbe & van der Donk, 1998; Tommos *et al.* 1999). Oxidized Trp and Tyr residues have been characterized spectroscopically in a large number of proteins, although direct evidence for their involvement in multistep tunneling reactions is hard to come by (Bollinger *et al.* 1991; Sucheta *et al.* 1998; Hofbauer *et al.* 2001).

The *Ru(bpy)<sub>2</sub>(im)(His)<sup>3+/2+</sup>* reduction potential ( $E^\circ = 1.0$  V *versus* NHE) (Chang *et al.* 1991a) may be high enough to oxidize Trp or Tyr residues in Ru–azurin. If the reactive Cu(I) center is replaced by redox-inert Zn(II) in the protein, however, we find that photogenerated holes in *Ru(bpy)<sub>2</sub>(im)(HisX)<sup>3+</sup>* complexes remain localized on the Ru center. The energy gap between the Ru(III) hole state and oxidized bridge states must therefore be greater than 75 meV ( $3 k_B T$  at 295 K). The fact that oxidized bridge states lie at higher energy than the Ru(III) hole does not rule out multistep tunneling; endergonic steps can be compensated for by favorable reactions later in a sequence. Endergonic reactions, however, become less effective as the temperature decreases, so that multistep tunneling with highly endergonic steps will exhibit a strong dependence on temperature. Our finding that the rate of Cu(I)→Ru(III) ET in *Ru(bpy)<sub>2</sub>(im)(His-X)–azurin* is nearly independent of temperatures between 240 and 300 K coupled with the observation that decreasing the temperature to 170 K produces a twofold increase in the ET rate demonstrate that multistep tunneling cannot explain long-range ET in Ru–azurin. Instead, the data shown in Figure 6 provide a calibration standard for superexchange-mediated electron tunneling in proteins.

The rates of high-driving-force ET reactions have been measured for more than 30 Ru (diimine)-labeled metalloproteins (Tables 1–5) (Gray & Winkler, 1996; Winkler *et al.* 1999;



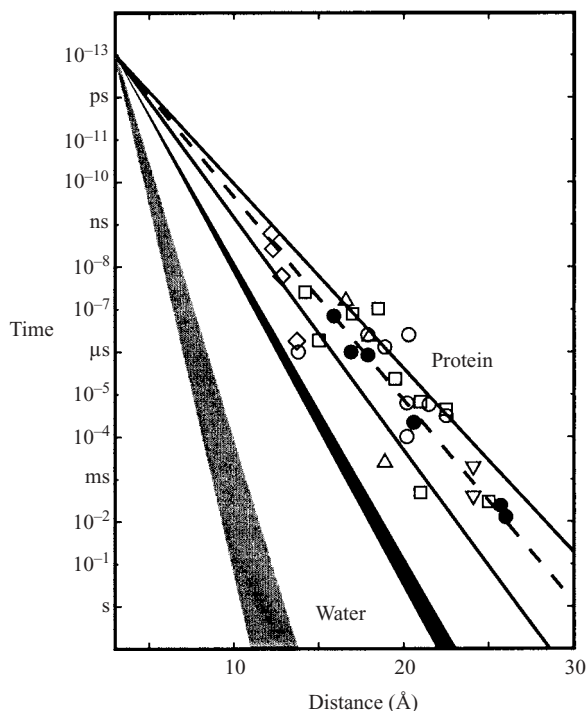


**Fig. 7.** Tunneling timetable for ET in Ru-modified proteins: azurin (●); cyt *c* (○); myoglobin (△); cyt *b*<sub>562</sub> (□); HiPIP (◇); and Fe:Zn-cyt *c* crystals (▽). The solid lines illustrate the tunneling pathway predictions for coupling along β-strands ( $\beta = 1.0 \text{ \AA}^{-1}$ ) and α-helices ( $\beta = 1.3 \text{ \AA}^{-1}$ ); the dashed line illustrates a  $1.1 \text{ \AA}^{-1}$  distance decay. Distance decay for electron tunneling through water is shown as a black wedge. Estimated distance dependence for tunneling through vacuum is shown as a grey wedge.

Babini *et al.* 2000). Only modest corrections are required to scale these rates to driving-force-optimized values, permitting comparisons of ET in different proteins. The results are summarized in the electron tunneling timetable of Figure 7. The reported distances are all metal-to-metal measures; in the case of metal clusters, the closest metal was chosen. Tunneling times range from a few nanoseconds (12.2-Å ET in the high-potential iron sulfur protein from *C. vinosum*) to 10 ms (26-Å ET in *P. aeruginosa* azurin).

The Ru-protein data-points are scattered around the Ru-azurin ( $\beta = 1.1 \text{ \AA}^{-1}$ ) exponential distance decay. More than 75% of the Ru-protein ET rates fall in a  $1.0\text{--}1.3 \text{ \AA}^{-1}$   $\beta$ -value zone. There is a tendency for researchers to hope that a simple rate/distance correlation will emerge from measurements of intramolecular protein ET rates. The data in Figure 7 clearly demonstrate that it is a tremendous oversimplification to define a canonical distance decay constant for electron tunneling in proteins. Rates at a single distance can differ by as much as a factor of  $10^3$  and D/A distances that differ by as much as 5 Å can produce identical rates! We regard the absence of a simple exponential distance dependence in the Ru-protein rate data as a reflection of the heterogeneity of the coupling medium. The efficiency of the coupling between redox centers is determined by the 3D structure of the intervening polypeptide. While the azurin β-barrel structure supports a relatively uniform distance decay, highly helical proteins (Mb, cyt *b*<sub>562</sub>) exhibit far more heterogeneous behavior. The lesson that emerges from our 30-year research program is that the protein fold is the key determinant of biological ET

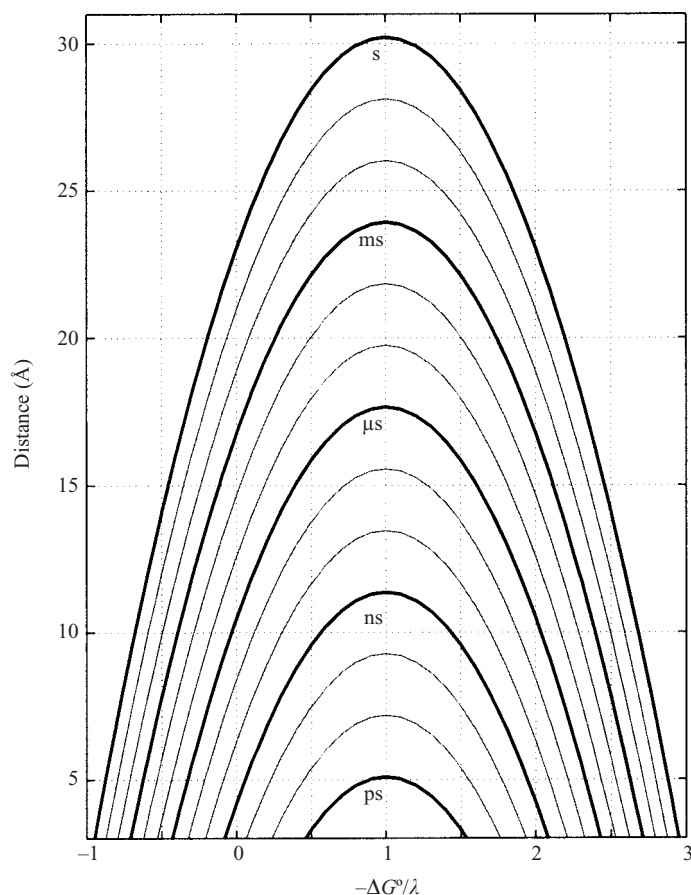


**Fig. 8.** Contour plot of tunneling time ( $1/\kappa_{\text{obs}}$ ) as a function of donor–acceptor distance ( $\beta = 1.1 \text{ \AA}^{-1}$ ) and driving force (in units of  $\lambda$ ;  $\kappa_{\text{B}} T/\lambda = 0.318$ ).

rates: it establishes the driving force, the reorganization energy, *and* the electronic coupling (Gray *et al.* 2000).

## 5. Multistep tunneling

Biological ET reactions typically proceed with very small releases of free energy. This efficient movement of charge helps retain the chemical potential of the transferring hole or electron. In order that ET does not become rate limiting in biological redox processes, millisecond or faster tunneling times are required. For low driving forces, this requirement sets the maximum center-to-center distance for biological tunneling reactions at  $\sim 20 \text{ \AA}$  (Fig. 8). Large assemblies of redox enzymes, however, often require that charges move over distances far greater than  $20 \text{ \AA}$  (Ramirez *et al.* 1995; Stubbe *et al.* 2003). Multiple tunneling steps are necessary to transport charge over longer distances (Page *et al.* 1999; Winkler *et al.* 1999). Semi-conductivity models of biological electron flow (Ye & Ladik, 1994; Iguchi, 1997; Herz *et al.* 2000; Sheu *et al.* 2002), first suggested by Szent-Györgyi (1941) over 60 years ago and continually cited today, are essentially multistep tunneling models. Multistep tunneling, particularly with endergonic steps, is a viable

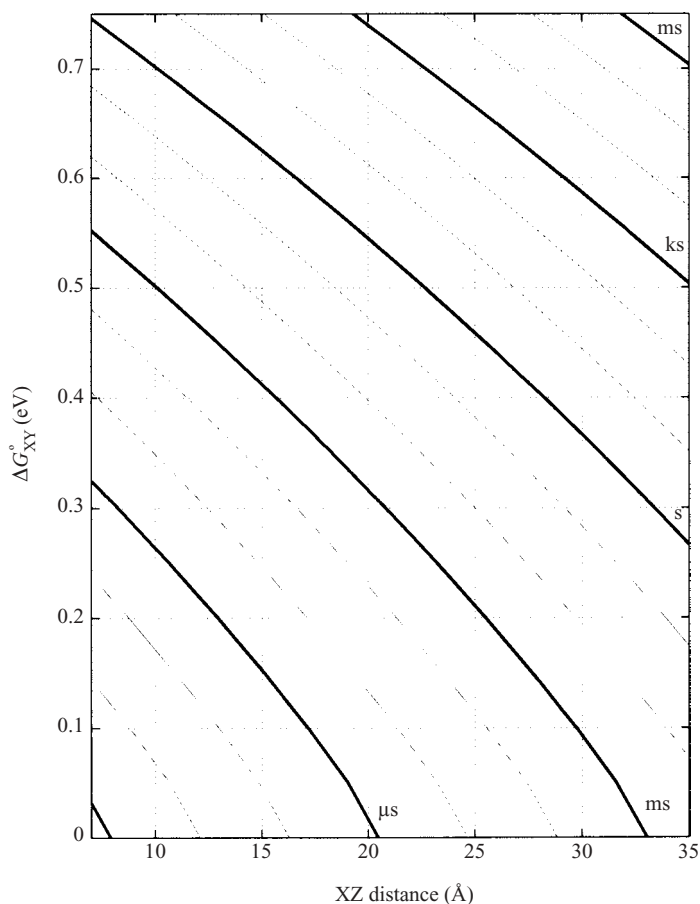


**Fig. 9.** Contour plot of lifetimes ( $1/k_{\text{obs}}$ ) for two-step, ergoneutral ( $-\Delta G_{\text{XZ}}^{\circ}=0$ ) tunneling [Eq. (11)] as a function of driving force for the  $\text{X} \rightleftharpoons \text{Y}$  step ( $-\Delta G_{\text{XY}}^{\circ}$ ) and distance between sites X and Z ( $r_{\text{XZ}}$ ,  $\beta=1.1 \text{ \AA}^{-1}$ ). Millisecond electron transport over  $30 \text{ \AA}$  is possible if the free-energy change for the first ET step ( $\Delta G_{\text{YZ}}^{\circ}$ ) is less than  $100 \text{ meV}$ .

method for delivering charges over long distances. But, in order to meet the critical demands of biological electron flow, careful positioning of redox centers and fine control of reaction driving forces are essential.

Modeling the kinetics of multistep tunneling processes is a straightforward problem that can be solved analytically without employing simplifying approximations. Using the well-defined properties of ET reactions [Eq. (1)], and the average distance dependence defined by Ru–protein tunneling timetables, it is possible to predict multistep tunneling rates for any set of driving-force, temperature, and distance parameters. Consider the two-step tunneling reaction defined in Eq. (11):



The general solution to the rate law for this process calls for bi-exponential production of Z, although under some circumstances the appearance of Z can be approximated by a single

exponential function. The objective of a long-range transport process is to get the charge from X to Z; we can compare different reaction conditions by defining an average time constant ( $\tau$ ) for the formation Z [Eq. (12)]:

$$\langle \tau \rangle = \int_0^\infty \frac{[Z]_t - [Z]_\infty}{[Z]_0 - [Z]_\infty} dt. \quad (12)$$

Taking a value of  $\lambda = 0.8$  eV for both tunneling reactions (i.e.  $X \rightarrow Y$  and  $Y \rightarrow Z$ ) and a distance decay constant of  $1.1 \text{ \AA}^{-1}$ , we can calculate the time dependence of the populations of all three reacting species for various values of  $\Delta G_{XY}^\circ$ ,  $\Delta G_{YZ}^\circ$ ,  $r_{XY}$ , and  $r_{YZ}$ . Results for the particular case in which  $\Delta G_{XY}^\circ = -\Delta G_{YZ}^\circ$  and  $r_{XY} = r_{YZ}$  are illustrated in Figure 9. This model approximates a biological electron-transport chain ( $\Delta G_{XZ}^\circ = 0$ ) reaction with a single endergonic step. Symmetrical placement of the redox centers produces the minimum transfer times. Transport across  $20 \text{ \AA}$  is  $10^4$  times faster than a single tunneling step at this distance and submillisecond transfers can be realized. For X–Z separations less than  $20 \text{ \AA}$ , endergonic intermediate steps as large as  $0.4\text{--}0.5$  eV will afford submillisecond transport times. An important conclusion is that multistep tunneling can facilitate electron flow over distances greater than  $25 \text{ \AA}$  in cases where the free-energy changes for endergonic intermediate steps are no greater than  $0.2$  eV.

## 6. Protein–protein reactions

In low ionic strength buffers, many proteins of opposite charge will form relatively tightly bound complexes (McLendon & Hake, 1992; McLendon *et al.* 1993; Nocek *et al.* 1996). With the aid of rapid triggering methods, it has been possible to measure rates of long-range ET between redox sites in these protein–protein complexes. In many complexes, there are multiple binding sites and is not uncommon to find that the ET kinetics often are regulated by the dynamics of conformational changes in the complex (Stemp & Hoffman, 1993; Pletneva *et al.* 2000). The usual interpretation is that surface diffusion of the two proteins produces a transient complex with significantly better electronic coupling and faster ET. Consequently, rates depend strongly on solvent viscosity rather than intrinsic ET parameters ( $\Delta G^\circ$ ,  $\lambda$ ,  $r$ ). A further complication associated with studies of protein–protein ET in solution is that binding sites and, hence, locations of redox cofactors, often are unknown. Issues of conformational change and structural ambiguity have been addressed recently with measurements of protein–protein ET kinetics in protein crystals (see below).

### 6.1 Hemoglobin (Hb) hybrids

Kinetics measurements on crystallographically characterized metal-substituted Hb hybrids provided some of the earliest insights into inter-protein ET rates (McGourty *et al.* 1983; Kuila *et al.* 1991). Because Hb is a very strongly bound complex of four polypeptide subunits, ET measurements are not complicated by the dynamical problems that plague interpretation of rates in more weakly bound complexes. Replacement of the native Fe center in the  $\beta$ -subunits of Hb with Zn or Mg creates the opportunity for photoinitiated ET reactions. The reacting metal centers in the Hb hybrids are separated by  $25 \text{ \AA}$  so that rates are relatively slow even at high driving forces. The time constant for ET from a triplet excited ZnPor in the  $\beta$ -subunit to an Fe(III) center in the  $\alpha$ -subunit is about  $16 \text{ ms}$  (McGourty *et al.* 1983). Extensive studies of temperature dependences of hybrid Hb ET rates led to the conclusion that the reorganization energy for these reactions

( $\lambda \sim 1$  eV) is dominated by outer-sphere contributions (Peterson-Kennedy *et al.* 1986; Dick *et al.* 1998). Measurements of ET rates in cryogenic glasses suggest that the polypeptide is the primary outer-sphere medium for the reaction and that bulk solvent reorganization does not play an important role in the reaction (Kuila *et al.* 1991). Moreover, it has been suggested that even at room temperature, the protein medium in Hb acts like a frozen glass (Dick *et al.* 1998). Results from measurements on Ru–azurin crystals also indicate that bulk solvent makes only a minor contribution to protein ET reorganization energies (Crane *et al.* 2001).

## 6.2 Cyt *c*/cyt *b*<sub>5</sub> complexes

The ET reaction between cyt *c* and cyt *b*<sub>5</sub> has been the subject of experimental and theoretical investigations for more than 40 years (Durham *et al.* 1995; Mauk *et al.* 1995). Modeling studies of both bimolecular and intramolecular ET between these proteins has been an active field of study. The detailed structural model proposed by Salemme in 1976 for the precursor complex of this protein pair stimulated a great deal of experimental work (Salemme, 1976). Careful spectroscopic studies revealed that these oppositely charged proteins form a stable 1:1 complex at low ionic strength [ $K_A = 8(3) \times 10^4 \text{ M}^{-1}$ , pH 7,  $\mu$  10 mM;  $K_A = 4(3) \times 10^6 \text{ M}^{-1}$ , pH 7,  $\mu$  1 mM] (Mauk *et al.* 1982).

McLendon & Miller (1985) employed a combination of photochemical and pulse-radiolytic methods to probe the driving-force dependence of heme–heme ET in this complex. The ET rates exhibited a near-Gaussian free-energy dependence, in excellent agreement with a 0.8-eV reorganization energy. The significance of this result is that, although this is a relatively low value of  $\lambda$  for ET between transition metal complexes in aqueous solution, it is by no means optimized. Most biological ET processes release less than 0.3 eV of free energy; with a 0.8-eV reorganization energy, rates will be 1–2 orders of magnitude below their maximum values.

Evidence for more complex ET processes came from studies in which photochemically generated reductants injected electrons into preformed Fe–cyt *b*<sub>5</sub>/Fe–cyt *c* complexes. In one study, the rate of *b*<sub>5</sub>→*c* ET ( $1.7 \times 10^3 \text{ s}^{-1}$ ) was reported to depend on viscosity and surface mutations (Qin *et al.* 1991). A later laser flash photolysis study found a rate-limiting second-order reduction of Fe–cyt *b*<sub>5</sub>/Fe–cyt *c* complexes and no sign of saturation, suggesting that the intra-complex ET rate was greater than  $10^4 \text{ s}^{-1}$  (Meyer *et al.* 1993).

Durham, Millett, and co-workers employed Ru-modified cyt *b*<sub>5</sub> and photochemical triggering methods to examine the kinetics of ET in cyt *b*<sub>5</sub>/*c* complexes (Meyer *et al.* 1993; Durham *et al.* 1995). Rapid intra-protein reduction (<100 ns) of Fe(III)–cyt *b*<sub>5</sub> by excited Ru(bpy)<sub>3</sub><sup>2+</sup> made it possible to probe *b*<sub>5</sub>→*c* ET kinetics. Two concentration-independent ET rates ( $4 \times 10^5 \text{ s}^{-1}$ ,  $3.4 \times 10^4 \text{ s}^{-1}$ ) were observed, suggesting that two cyt *b*<sub>5</sub>/*c* species are present in solution. Studies of ionic strength dependences and the effects of mutations suggest that the slower Fe(III)–cyt *c* reduction phase may be limited by conformational changes within one of the complexes (Durham *et al.* 1995).

## 6.3 Cyt *c*/cyt *c* peroxidase complexes

Cyt *c* peroxidase (ccp) catalyzes the two-electron reduction of H<sub>2</sub>O<sub>2</sub> by ferrocycytochrome *c*. Peroxide reacts rapidly with the resting ferric form of ccp to produce a species referred to as compound I, which contains a ferryl [Fe(IV)O<sup>2+</sup>] heme and a protein radical located on Trp191. The ET reactions involving these physiological redox partners have been studied in great detail (Nocek *et al.* 1996). At low ionic strength, acidic ccp and basic cyt *c* will form a stable complex.

A model of a 1:1 complex, based on the crystal structures of the two independent proteins, was proposed by Poulos & Kraut (1980). Twelve years later, Pelletier & Kraut (1992) reported the crystal structure of a 1:1 complex of the two yeast proteins. Interestingly, the complex between yeast ccp and horse cyt *c* exhibited a slightly different structure. Analysis of the yeast/yeast complex suggested an electronic coupling pathway from the cyt *c* heme to the ccp heme via Trp191. On the basis of these crystallographic results, Pelletier and Kraut argued that ccp and cyt *c* form a highly specific 1:1 ET complex.

Hoffman and co-workers have employed metal-substituted ccp and cyt *c* to explore the ET kinetics between these two proteins (Nocek *et al.* 1996). Results from four-dimensional quenching studies, temperature and ionic strength dependences, species variations, and electrostatic modeling provide compelling evidence for two distinct cyt *c*-binding sites on ccp. The higher affinity binding site is the locus for Trp191 radical reduction by cyt *c*. Heme (ccp) reduction by cyt *c* can occur from either the high- or low-affinity binding site but, when exchange between the two is rapid, reduction from the low-affinity site dominates (Nocek *et al.* 1996). These studies of ccp/cyt *c* ET, as well as those of cyt *b<sub>5</sub>/c*, reveal the considerable mechanistic complexity of protein–protein ET processes.

#### 6.4 Zn–cyt *c*/Fe–cyt *c* crystals

Studies of ccp/cyt *c* and cyt *b<sub>5</sub>/c* reactions highlight the difficulty of extracting ET parameters when donors and acceptors are not held at fixed distances and orientations. At least three elementary steps are required to complete a redox reaction between soluble proteins: (i) formation of an active donor–acceptor complex; (ii) electron tunneling within the donor–acceptor complex; and (iii) dissociation of the oxidized and reduced products. Because the dynamics of the first and third steps obscure the electron-tunneling reaction, experimental studies must focus on ET reactions within protein–protein complexes that form at low ionic strength. It has been difficult to interpret the results, however, as neither the donor–acceptor docking geometries nor the conformations of these complexes are known with certainty.

Crystals containing photoactivatable donors and acceptors at specific lattice sites are ideal media for investigating tunneling between proteins. In crystal lattices of tuna cyt *c*, chains of cyt *c* molecules form helices with a 24.1-Å separation between neighboring metal centers (Tezcan *et al.* 2001). All other metal–metal distances in the lattice are greater than 30 Å. Thus, the heme groups can be treated as ordered in a one-dimensional chain, separated by identical protein and solvent media. By doping Zn–cyt *c* into this lattice, inter-protein ET was probed using laser-flash transient spectroscopy. ET from the triplet-excited ZnPor to a neighboring Fe(III)–cyt *c* proceeded with a rate constant of  $4(1) \times 10^2 \text{ s}^{-1}$ ; the rate of charge recombination was about five times faster [ $2.0(5) \times 10^3 \text{ s}^{-1}$ ] (Tezcan *et al.* 2001).

Rapid relay of electrons involving at least one soluble redox enzyme requires the formation of short-lived, weakly bound protein–protein complexes. The recognition sites between proteins in such complexes tend to be smaller ( $<1200 \text{ Å}^2$ ) and include more water molecules than the interfaces between subunits in oligomeric proteins (Lo Conte *et al.* 1999). The inter-protein interactions in crystals of tuna cyt *c* involve relatively few contacts: 760 Å<sup>2</sup> of surface area is buried in an interface with 31 van der Waals contacts ( $3.2 \leq d \leq 3.9 \text{ Å}$ ) and 16 water molecules (3 of which form bridging hydrogen bonds across the interface) but only one direct hydrogen bond bridging the two proteins. Indeed, the cyt *c*–cyt *c* interface is reminiscent of that between the natural redox partners, cyt *c* and ccp (770 Å<sup>2</sup>) (Pelletier & Kraut, 1992), and may be typical

of the interaction zones for soluble redox proteins. The Zn–Fe separation in doped tuna cyt *c* crystals is similar to that in Zn–Fe–Hb hybrids (24.7 Å, T state), although the tetrameric heme protein has many more contacts between subunits and a greater atom density at the interface. Nevertheless,  $^*\text{ZnPor} \rightarrow \text{Fe(III)}$  and  $\text{Fe(II)} \rightarrow \text{ZnPor}^{+\bullet}$  ET rates in Hb hybrids (McGourty *et al.* 1983) and Zn-doped tuna cyt *c* crystal are quite similar and fall well within the range that has been established in studies of Ru-modified proteins (Gray & Winkler, 1996; Winkler *et al.* 1999). The protein crystal ET data demonstrate that small interaction zones of low density are quite effective in mediating inter-protein redox reactions.

## 7. Photosynthesis and respiration

Aerobic organisms derive most of the energy needed for life processes by the burning of food-stuffs with molecular oxygen in air (Ramirez *et al.* 1995). In the first part of the respiratory process, hydrogen atoms are extracted from organic molecules. The hydrogen carriers are later regenerated in the respiratory chain located in cell organelles, mitochondria, or, in bacteria, in the cell membrane. These chains consist of a series of membrane-bound protein complexes in which the hydrogen atoms are split into protons and electrons. The electrons are passed down the chain and reduce molecular oxygen to water, whereas protons are left behind on one specific side of the membrane. In addition, the electron current through the chain is coupled to a pumping of additional protons from water to the same side of the membrane (Brzezinski & Larsson, 2003). The two proton currents lead to an increased positive charge and decreased pH on this side. The resulting electrochemical potential across the membrane drives the synthesis of ATP, the universal energy currency of living cells.

Photosynthesis is the natural complement to respiration. Photons from the sun induce charge separation in a membrane-bound redox chain, ultimately producing a transmembrane potential for ATP synthesis. In green plants, algae, and cyanobacteria, the photogenerated holes oxidize water to oxygen. The photochemically generated reducing equivalents produce NADPH that, along with ATP, is used in carbon dioxide fixation.

Highly optimized ET reactions are essential for the operation of these biochemical machines.

### 7.1 Photosynthetic reaction centers (PRCs)

Bacterial PRCs have been among the most actively studied ET proteins since DeVault and Chance first measured *C. vinosum* tunneling rates in the early 1960s (De Vault & Chance, 1966; De Vault *et al.* 1967). In many cases, measurements of ET kinetics preceded determination of the 3D structure of the membrane-bound protein assembly. It was not until the X-ray crystal structure determinations of the *Rhodospseudomonas (Rps.) viridis* (Deisenhofer *et al.* 1985, 1995) and *Rhodobacter (Rb.) sphaeroides* (Allen *et al.* 1987; Komiya *et al.* 1988) PRCs that distances could be assigned to specific rate constants.

The evaluation of driving forces and reorganization energies in PRCs has been problematic. The PRC redox cofactors are embedded among an array of  $\alpha$ -helices spanning a lipid bilayer. Direct measurement of these cofactor redox potentials is a formidable challenge (Alegria & Dutton, 1991a, b). Furthermore, electrostatic interactions among redox cofactors make it difficult to extract reaction driving forces from midpoint potentials (Gunner & Honig, 1991; Gunner *et al.* 1996; Baymann & Rappaport, 1998). In addition, the ET reactions involving quinones are complicated by the kinetics and energetics of proton transfer. Modifying reaction-driving



forces is difficult because the redox centers are intrinsic protein cofactors. Site-directed mutation of residues near redox cofactors has proved to be an effective means of varying redox potentials, providing driving-force data for selected PRC ET reactions (Chen *et al.* 2000; Lin *et al.* 1994a).

Charge separation in PRCs arises from a series of highly optimized ET processes. The primary photochemical event involves 2-ps ET over 17.8 Å from an electronically excited chlorophyll special pair (\*P) to a pheophytin acceptor (Kirmaier & Holten, 1987). The rate of this reaction increases by a factor of approximately 2 as the temperature is lowered from 295 to 4 K. The absence of thermal activation indicates that the reorganization energy for \*P→BPh ET must be close to the driving force (0.2 eV). The reduced pheophytin delivers an electron to a quinone (Q<sub>A</sub>) 14.5 Å away in 100 ps. This productive reaction is 500 times faster than charge recombination with the hole in the bacteriochlorophyll special pair (P<sup>•+</sup>). In 100 ps, approximately half of the 1.3 eV excitation energy of \*P has been used to produce a 28.7 Å charge separation (Franzen *et al.* 1993).

The hole in the bacteriochlorophyll special pair is filled by ET from a cytochrome. In *Rps. viridis*, the cytochrome donor is tightly bound to the PRC at the membrane surface. This subunit contains four hemes in a nearly linear array oriented perpendicular to the membrane (Deisenhofer *et al.* 1985, 1995). The reduction potentials of the hemes alternate from high ( $\geq 250$  mV *versus* NHE) to low ( $\leq 50$  mV) as the distance from P increases (Alegria & Dutton, 1991b; Baymann & Rappaport, 1998). The heme closest to the special pair, cyt  $\epsilon_{559}$ , has the highest potential and fills the P<sup>•+</sup> hole in approximately  $\sim 200$  ns (Shopes *et al.* 1987; Ortega & Mathis, 1993). The next well-characterized process is ET from cyt  $\epsilon_{556}$  to cyt  $\epsilon_{559}$  in  $\sim 2$   $\mu$ s over a distance of 27.9 Å (Shopes *et al.* 1987; Ortega & Mathis, 1993).

In *Rb. sphaeroides*, P<sup>•+</sup> is reduced by a soluble single heme protein, cyt  $\epsilon_2$ . Several *Rb. sphaeroides* PRC mutants with altered P<sup>•+</sup>/<sup>0</sup> potentials have been prepared. In all,  $E^\circ(\text{P}^{\bullet+}/^0)$  values range from a low of 0.410 V to a high of 0.765 V *versus* NHE (the wild-type value is 0.505 V) (Lin *et al.* 1994a). A driving-force study of Fe(II)→P<sup>•+</sup> ET in cyt  $\epsilon_2$ /PRC complexes gave  $\lambda = 0.5$  eV (Lin *et al.* 1994b). Global analysis of temperature *and* driving-force dependences of these ET rates indicated that  $\lambda = 0.96 \pm 0.07$  eV, and  $H_{AB}$  values were not constant for all of the mutants (Venturoli *et al.* 1998). The variation of  $\Delta G^\circ$  with temperature, however, was not taken into account in this analysis and it is possible that the uncertainty in  $\lambda$  is greater than the reported 70 meV. The kinetics of ET from cyt  $\epsilon_2$  to P<sup>•+</sup> in the PRC from *Rb. sphaeroides* have been measured in structurally characterized crystals (Axelrod *et al.* 2002). The rate ( $1.1 \times 10^6$  s<sup>-1</sup>), driving force (0.16 eV), and donor–acceptor distance (21.2 Å) are quite similar to those for ET from cyt  $\epsilon_{559}$  to P<sup>•+</sup> in *Rps. viridis*.

Photosynthesis works because charge separation is more efficient than energy-wasting charge recombination. By blocking appropriate steps in the charge-separation sequence, it has been possible to determine the rates of PRC charge-recombination reactions. The near-linear arrangement of redox cofactors forms a redox potential gradient that favors short-range charge-separation reactions. In all cases, charge recombinations are many orders of magnitude slower than competing charge-separation reactions (Franzen *et al.* 1993).

Many of the PRC ET reactions exhibit only modest variations with temperature. The rate of the primary photochemical event increases at cryogenic temperature (Kirmaier & Holten, 1987). Several other reaction rates decrease by only small factors when temperatures are lowered (Venturoli *et al.* 1998). For charge separation, this behavior can be attributed to driving-force-optimized reactions.

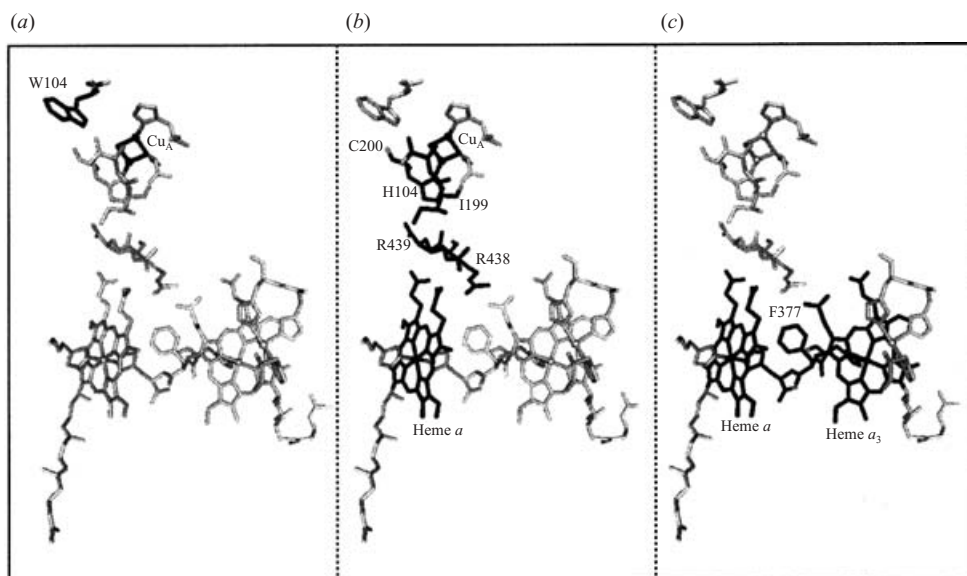


**Fig. 10.** Electron tunneling pathways in CcO. Residues involved in the specified pathways are labeled and appear in black: (a) cyt *c* to Cu<sub>A</sub>; (b) Cu<sub>A</sub> to heme *a*; (c) heme *a* to heme *a*<sub>3</sub>.

## 7.2 Cyt *c* oxidase (CcO)

In the terminal reaction of the respiratory chain, membrane-bound CcO removes electrons from soluble cyt *c* and passes them on to O<sub>2</sub> (Ramirez *et al.* 1995). CcO is a multisubunit membrane-bound enzyme with four redox cofactors (Cu<sub>A</sub>, cyt *a*, cyt *a*<sub>3</sub>, Cu<sub>B</sub>). The locations of these metal complexes in CcO were revealed in the 1990s by the X-ray crystal structures of bacterial (Iwata *et al.* 1995) and bovine enzymes (Tsukihara *et al.* 1995; Yoshikawa *et al.* 1998). Cu<sub>A</sub>, a binuclear Cu site with bridging S(Cys) atoms, is the primary electron acceptor from soluble cyt *c*. Studies with Ru-modified cyt *c* reveal rapid ( $6 \times 10^4 \text{ s}^{-1}$ ) (Geren *et al.* 1995) electron injection from Fe(II) into Cu<sub>A</sub> at low driving force ( $\Delta G^\circ = -0.03 \text{ eV}$ ) (Pan *et al.* 1993). Modeling suggests that cyt *c* binds to the bovine enzyme at an acidic patch on subunit II with an Fe–Cu distance of 17.8 Å (Roberts & Pique, 1999). The cyt *c* heme is within 3.3 Å of the Trp104 (subunit II) indole ring, a residue that appears from mutagenesis experiments to be critical for rapid cyt *c*/Cu<sub>A</sub> ET. Solomon and co-workers have identified a possible electron tunneling path from this cyt *c*-binding site through Trp104 to the bridging S(Cys200) ligand on Cu<sub>A</sub> (Fig. 10) (George *et al.* 2001).

The 19.6-Å ET from Cu<sub>A</sub> to cyt *a* proceeds rapidly at low driving force ( $1.8 \times 10^4 \text{ s}^{-1}$ ;  $\Delta G^\circ = -0.05 \text{ eV}$ ) (Geren *et al.* 1995). Three electronic coupling pathways have been considered for this reaction (Fig. 10). Ramirez (Ramirez *et al.* 1995), Regan (Regan *et al.* 1998), and Solomon (Gamelin *et al.* 1998; George *et al.* 2001) have identified a coupling route that proceeds from Cu<sub>A</sub> ligand His204 (subunit II) across one hydrogen bond to Arg438 (subunit I) [H204(Nε)–R438(O), 3.36 Å], and another H-bond (2.95 Å) from the Arg438 N-amide to the cyt *a* heme propionate. Based on a tunneling currents analysis, Stuchebrukhov suggested a slightly different Cu<sub>A</sub>–cyt *a* coupling route through His204 (Medvedev *et al.* 2000). Both Solomon and Stuchebrukhov argued that, owing to strong Cu–S(Cys) electronic interactions, pathways involving the bridging Cys residues are important for mediating coupling even though they involve more bonds than

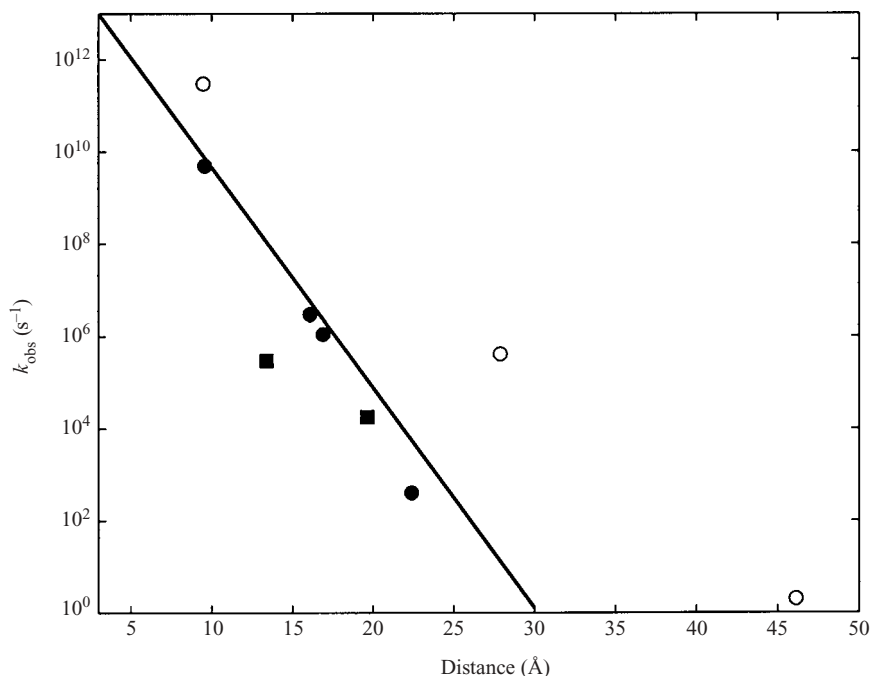


**Fig. 11.** Distance dependence of *observed* ET rates in CcO (■) and the PRC (●, ○). The open symbols correspond to processes where multistep tunneling may be involved. The solid line shows the average distance dependence found for driving-force-optimized ET in Ru-modified proteins ( $\beta = 1.1 \text{ \AA}^{-1}$ ).

the His204 route. Solomon originally proposed a Cys196/Tyr440/Arg438/heme-propionate (cyt *a*) pathway (Williams *et al.* 1997; Gamelin *et al.* 1998). Subsequent analysis by Stuchebrukhov (Medvedev *et al.* 2000) and Solomon (George *et al.* 2001) indicated that the sequence Cys200/Ile199/Arg439/heme-propionate (cyt *a*) is the dominant coupling route between  $\text{Cu}_A$  and cyt *a*.

Both Regan (Regan *et al.* 1998) and Stuchebrukhov (Medvedev *et al.* 2000) have analyzed the coupling between cyt *a* and cyt  $a_3$  (Fig. 10). The earlier analysis revealed three nearly equivalent coupling routes between the two hemes involving the axial His residues [His378(cyt *a*), His376(cyt  $a_3$ )]. One pathway proceeds through the intervening Phe377 residue; the other two involve a hydrogen bond between His378 and Val374. From Ala375, one pathway goes directly to His376 and the other involves a hydrogen bond to Tyr372 (which is hydrogen bonded to His376). Stuchebrukhov also identified three major cyt *a*/cyt  $a_3$  pathways: one is the direct jump from heme *a* to heme  $a_3$ ; one has the aromatic ring of Phe377 as the only intermediate group; and the third involves His378 and the Phe377 aromatic ring. In spite of the similarity in  $\text{Cu}_A$ –cyt *a* (19.6 Å) and  $\text{Cu}_A$ –cyt  $a_3$  (22.4 Å) distances, neither Regan (Regan *et al.* 1998) nor Stuchebrukhov (Medvedev *et al.* 2000) found a significant coupling pathway between the  $\text{Cu}_A$  center and cyt  $a_3$ .

## 8. Concluding remarks

It is interesting to consider measured rates of electron tunneling in CcO and photosynthetic reaction centers in the context of results obtained with Ru-modified proteins (Fig. 11). The solid line in the figure corresponds to the average distance dependence of driving-force-optimized

ET rates in Ru proteins ( $\beta = 1.1 \text{ \AA}^{-1}$ ;  $10^{13} \text{ s}^{-1}$  intercept). The fact that most of the observed tunneling rates in CcO and the PRC lie near to or *above* this line indicates that the natural ET reactions are highly optimized, both in terms of reorganization energy and electronic coupling. Three of the *Rps. viridis* PRC reactions are at least 2 orders of magnitude faster than would be expected for activationless ET: the initial charge separation event; ET from cyt  $\epsilon_{556}$  to cyt  $\epsilon_{559}$ ; and charge recombination from reduced  $Q_A$  to cyt  $\epsilon_{559}$ . These unusually high ET rates may signal the presence of multistep tunneling processes (Kirmaier & Holten, 1987; Page *et al.* 1999; Axelrod *et al.* 2002). It is interesting that neither the  $Q_A^- \rightarrow P^+$  nor the  $Q_A^- \rightarrow \text{cyt } \epsilon_{559}$  charge-recombination reaction is unusually slow. This contrasts with the  $BPh^- \rightarrow P^+$  reaction, which is  $10^3$  times slower than expected for a driving-force-optimized process at the same distance (Franzen *et al.* 1993). Inverted driving-force behavior may be responsible for retarding  $BPh^- \rightarrow P^+$  ET, but multistep tunneling may nullify its effects in the longer-range reactions. The rate of ET from  $Cu_A$  to cyt *a* in CcO is close to that expected for an optimized reaction, yet the reaction driving force is just 50 meV. Clearly, both the reorganization energy and the electronic coupling pathway in CcO have been finely tuned to achieve a high level of electron-transport efficiency.

## 9. Acknowledgments

We thank Peter Wolynes for encouragement and helpful discussions. Our work is supported by the National Institutes of Health, the National Science Foundation, and the Arnold and Mabel Beckman Foundation.

## 10. References

- ADMAN, E. T. (1991). Copper protein structures. *Advances in Protein Chemistry* **42**, 145–197.
- ADMAN, E. T. & JENSEN, L. H. (1981). Structural features of azurin at 2.7 Å resolution. *Israel Journal of Chemistry* **21**, 8–12.
- ALEGRIA, G. & DUTTON, P. L. (1991a). I. Langmuir–Blodgett monolayer films of bacterial photosynthetic membranes and isolated reaction centers: preparation, spectrophotometric and electrochemical characterization. *Biochimica et Biophysica Acta* **1057**, 239–257.
- ALEGRIA, G. & DUTTON, P. L. (1991b). II. Langmuir–Blodgett monolayer films of the *Rhodospseudomonas viridis* reaction center: determination of the order of the hemes in the cytochrome *c* subunit. *Biochimica et Biophysica Acta* **1057**, 258–272.
- ALLEN, J. P., FEHER, G., YEATES, T. O., KOMIYA, H. & REES, D. C. (1987). Structure of the reaction center from *Rhodobacter sphaeroides* R-26 – the cofactors. *Proceedings of the National Academy of Sciences USA* **84**, 5730–5734.
- AXELROD, H. L., ABRESCH, E. C., OKAMURA, M. Y., YEH, A. P., REES, D. C. & FEHER, G. (2002). X-ray structure determination of the cytochrome  $c_2$ : reaction center ET complex from *Rhodobacter sphaeroides*. *Journal of Molecular Biology* **319**, 501–515.
- BABINI, E., BERTINI, I., BORSARI, M., CAPOZZI, F., LUCHINAT, C., ZHANG, X., MOURA, G. L. C., KURNIKOV, I. V., BERATAN, D. N., PONCE, A., DI BILIO, A. J., WINKLER, J. R. & GRAY, H. B. (2000). Bond-mediated electron tunneling in ruthenium-modified high-potential iron-sulfur protein. *Journal of the American Chemical Society* **122**, 4532–4533.
- BALABIN, I. A. & ONUCHIC, J. N. (1998). A new framework for electron-transfer calculations – beyond the *pathways*-like models. *Journal of Physical Chemistry (B)* **102**, 7497–7505.
- BATTISTUZZI, G., BORSARI, M., COWAN, J. A., RANIERI, A. & SOLA, M. (2002). Control of cytochrome *c* redox potential: axial ligation and protein environment effects. *Journal of the American Chemical Society* **124**, 5315–5324.
- BATTISTUZZI, G., BORSARI, M. & SOLA, M. (2001). Medium and temperature effects on the redox chemistry of cytochrome *c*. *European Journal of Inorganic Chemistry*, 2989–3004.
- BATTISTUZZI, G., BORSARI, M., SOLA, M. & FRANIA, F. (1997). Redox thermodynamics of the native and alkaline forms of eucaryotic and bacterial class I cytochromes *c*. *Biochemistry* **36**, 16247–16258.
- BAYMANN, F. & RAPPAPORT, F. (1998). Electrostatic interactions at the donor side of the photosynthetic reaction

- center of *Rhodospseudomonas viridis*. *Biochemistry* **37**, 15320–15326.
- BERATAN, D. N., BETTS, J. N. & ONUCHIC, J. N. (1991). Protein ET rates set by the bridging secondary and tertiary structure. *Science* **252**, 1285–1288.
- BERATAN, D. N., BETTS, J. N. & ONUCHIC, J. N. (1992). Tunneling pathway and redox-state dependent electronic couplings at nearly fixed distance in electron-transfer proteins. *Journal of Physical Chemistry* **96**, 2852–2855.
- BERATAN, D. N. & ONUCHIC, J. N. (1989). Electron tunneling pathways in proteins: influences on the transfer rate. *Photosynthesis Research* **22**, 173–186.
- BERATAN, D. N., ONUCHIC, J. N. & HOPFIELD, J. J. (1987). Electron tunneling through covalent and noncovalent pathways in proteins. *Journal of Chemical Physics* **86**, 4488–4498.
- BIXLER, J., BAKKER, G. & MCLENDON, G. (1992). Electrochemical probes of protein folding. *Journal of the American Chemical Society* **114**, 6938–6939.
- BJERRUM, M. J., CASIMIRO, D. R., CHANG, I.-J., DI BILIO, A. J., GRAY, H. B., HILL, M. G., LANGEN, R., MINES, G. A., SKOV, L. K., WINKLER, J. R. & WUTKE, D. S. (1995). Electron transfer in ruthenium-modified proteins. *Journal of Bioenergetics and Biomembranes* **27**, 295–302.
- BOLLINGER JR., J. M., EDMONDSON, D. E., HUYNH, B. H., FILLEY, J., NORTON, J. R. & STUBBE, J. (1991). Mechanism of assembly of the tyrosyl radical-dinuclear iron cluster cofactor of ribonucleotide reductase. *Science* **253**, 292–298.
- BROWN, G. M. & SUTIN, N. (1979). A comparison of the rates of electron exchange reactions of ammine complexes of ruthenium(II) and -(III) with the predictions of adiabatic, outer-sphere electron transfer models. *Journal of the American Chemical Society* **101**, 883–892.
- BRUNSCHWIG, B. S. & SUTIN, N. (1987). Rate-constant expressions for nonadiabatic electron-transfer reactions. *Comments on Inorganic Chemistry* **6**, 209–235.
- BRUNSCHWIG, B. S. & SUTIN, N. (1989). Directional electron transfer: conformational interconversions and their effects on observed electron-transfer rate constants. *Journal of the American Chemical Society* **111**, 7454–7465.
- BRZEZINSKI, P. & LARSSON, G. (2003). Redox-driven proton pumping by heme-copper oxidases. *Biochimica et Biophysica Acta – Bioenergetics* **1605**, 1–13.
- CALCATERRA, L. T., CLOSS, G. L. & MILLER, J. R. (1983). Intramolecular electron transfer in radical ions over long distances across rigid saturated hydrocarbon spacers. *Journal of the American Chemical Society* **105**, 670–671.
- CASIMIRO, D. R., RICHARDS, J. H., WINKLER, J. R. & GRAY, H. B. (1993). Electron transfer in ruthenium-modified cytochromes *c*.  $\sigma$ -Tunneling pathways through aromatic residues. *Journal of Physical Chemistry* **97**, 13073–13077.
- CHANCE, B. & WILLIAMS, G. R. (1956). The respiratory chain and oxidative phosphorylation. *Advances in Enzymology* **17**, 65–134.
- CHANG, I.-J., GRAY, H. B. & WINKLER, J. R. (1991a). High-driving-force electron transfer in metalloproteins: intramolecular oxidation of ferrocycytochrome *c* by Ru(2,2'-bipyridine)<sub>2</sub>(imidazole)(histidine-33)<sup>3+</sup>. *Journal of the American Chemical Society* **113**, 7056–7057.
- CHANG, T. K., IVERSON, S. A., RODRIGUES, C. G., KISER, C. N., LEW, A. Y., GERMANAS, J. P. & RICHARDS, J. H. (1991b). Gene synthesis, expression and mutagenesis of the blue copper proteins azurin and plastocyanin. *Proceedings of the National Academy of Sciences USA* **88**, 1325–1329.
- CHEN, I.-P., PATHIS, P., KOEPKE, J. & MICHEL, H. (2000). Uphill electron transfer in the tetraheme cytochrome subunit of the *Rhodospseudomonas viridis* photosynthetic reaction center: evidence from site directed mutagenesis. *Biochemistry* **39**, 3592–3602.
- CHURG, A. K. & WARSH, A. (1986). Control of the redox potential of cytochrome *c* and microscopic dielectric effects in proteins. *Biochemistry* **25**, 1675–1681.
- CLOSS, G. L. & MILLER, J. R. (1988). Intramolecular long-distance electron transfer in organic molecules. *Science* **240**, 440–447.
- CRANE, B. R., DI BILIO, A. J., WINKLER, J. R. & GRAY, H. B. (2001). Electron tunneling in single crystals of *Pseudomonas aeruginosa* azurins. *Journal of the American Chemical Society* **123**, 11623–11631.
- CREUTZ, C. & SUTIN, N. (1977). Vestiges of the 'inverted region' for highly exergonic electron-transfer reactions. *Journal of the American Chemical Society* **99**, 241–243.
- DAVIS, W. B., RATNER, M. A. & WASIELEWSKI, M. R. (2002). Dependence of electron transfer dynamics in wire-like bridge molecules on donor-bridge energetics and electronic interactions. *Chemical Physics* **281**, 333–346.
- DE VAULT, D. & CHANCE, B. (1966). Studies of photosynthesis using a pulsed laser. I. Temperature dependence of cytochrome oxidase rate in chromatium. Evidence for tunneling. *Biophysical Journal* **6**, 825–846.
- DE VAULT, D., PARKES, J. H. & CHANCE, B. (1967). Electron tunnelling in cytochromes. *Nature* **215**, 642–644.
- DEFELIPPIS, M. R., MURTHY, C. P., FARAGGI, M. & KLAPPER, M. H. (1989). Pulse radiolytic measurement of redox potentials: the tyrosine and tryptophan radicals. *Biochemistry* **28**, 4847–4853.
- DEISENHOFER, J., EPP, O., MIKI, K., HUBER, R. & MICHEL, H. (1985). Structure of the protein subunits in the photosynthetic reaction center of *Rhodospseudomonas viridis* at 3 Å resolution. *Nature* **318**, 618–624.
- DEISENHOFER, J., EPP, O., SINNING, I. & MICHEL, H. (1995). Crystallographic refinement at 2.3 Å resolution and refined model of the photosynthetic reaction center from *Rhodospseudomonas viridis*. *Journal of Molecular Biology* **246**, 429–457.



- DI BILIO, A. J., HILL, M. G., BONANDER, N., KARLSSON, B. G., VILLAHERMOSA, R. M., MALMSTRÖM, B. G., WINKLER, J. R. & GRAY, H. B. (1997). Reorganization energy of blue copper: effects of temperature and driving force on the rates of electron transfer in ruthenium- and osmium-modified azurins. *Journal of the American Chemical Society* **119**, 9921–9922.
- DICK, L. A., Malfant, I., Kuila, D., Nebolsky, S., Nocek, J. M., Hoffman, B. M. & Ratner, M. A. (1998). Cryogenic electron tunneling within mixed-metal hemoglobin hybrids: protein glassing and electron-transfer energetics. *Journal of the American Chemical Society* **120**, 11401–11407.
- DURHAM, B., FAIRRIIS, J. L., McLEAN, M., MILLETT, F., SCOTT, J. R., SLIGAR, S. G. & WILLIE, A. (1995). Electron transfer from cytochrome  $b_5$  to cytochrome  $c$ . *Journal of Bioenergetics and Biomembranes* **27**, 331–340.
- ELIAS, H., CHOU, M. H. & WINKLER, J. R. (1988). Electron-transfer kinetics of Zn-substituted cytochrome  $c$  and its  $\text{Ru}(\text{NH}_3)_5(\text{histidine-33})$  derivative. *Journal of the American Chemical Society* **110**, 429–434.
- EVANS, M. G. & GERGELY, J. (1949). A discussion of the possibility of bands of energy levels in proteins. Electronic interactions in non bonded systems. *Biochimica et Biophysica Acta* **3**, 188–197.
- EVENSON, J. W. & KARPLUS, M. (1993). Effective coupling in biological electron transfer: exponential or complex distance dependence? *Science* **262**, 1247–1249.
- FOX, L. S., KOZIK, M., WINKLER, J. R. & GRAY, H. B. (1990). Gaussian free-energy dependence of electron-transfer rates in iridium complexes. *Science* **247**, 1069–1071.
- FRANZEN, S., GOLDSTEIN, R. F. & BOXER, S. G. (1993). Distance dependence of electron-transfer reactions in organized systems: the role of superexchange and non-condon effects in photosynthetic reaction centers. *Journal of Physical Chemistry* **97**, 3040–3053.
- FREED, K. F. (1983). Role of intramolecular vibrational relaxation on electron transfer rates – application to pentaammineruthenium(III)(histidine-33)-ferricytochrome  $c$ . *Chemical Physics Letters* **97**, 489–493.
- GAMELIN, D. R., RANDALL, D. W., HAY, M. T., HOUSER, R. T., MULDER, T. C., CANTERS, G. W., DE VRIES, S., TOLMAN, W. B., LU, Y. & SOLOMON, E. I. (1998). Spectroscopy of mixed-valence  $\text{Cu}_A$ -type centers: ligand-field control of ground-state properties related to electron transfer. *Journal of the American Chemical Society* **120**, 5246–5263.
- GEORGE, S. D., METZ, M., SZILAGYI, R. K., WANG, H., CRAMER, S. P., LU, Y., TOLMAN, W. B., HEDMAN, B., HODGSON, K. O. & SOLOMON, E. I. (2001). A quantitative description of the ground-state wave function of  $\text{Cu}_A$  by X-ray absorption spectroscopy: comparison to plastocyanin and relevance to electron transfer. *Journal of the American Chemical Society* **123**, 5757–5767.
- GEREN, L. M., BEASLEY, J. R., FINE, B. R., SAUNDERS, A. J., HIBDON, S., PIELAK, G. J., DURHAM, B. & MILLETT, F. (1995). Design of a ruthenium-cytochrome  $c$  derivative to measure electron transfer to the initial acceptor in cytochrome  $c$  oxidase. *Journal of Biological Chemistry* **270**, 2466–2472.
- GRAY, H. B., MALMSTRÖM, B. G. & WILLIAMS, R. J. P. (2000). Copper coordination in blue proteins. *Journal of Biological Inorganic Chemistry* **5**, 551–559.
- GRAY, H. B. & WINKLER, J. R. (1996). Electron transfer in proteins. *Annual Review of Biochemistry* **65**, 537–561.
- GRAY, H. B. & WINKLER, J. R. (2001). Electron transfer in biological systems. In *Electron Transfer in Chemistry*, vol. III (ed. V. Balzani), pp. 1–175. Weinheim: Wiley-VCH.
- GRAY, H. B. & WINKLER, J. R. (2003). Heme protein dynamics: electron tunneling and redox triggered folding. In *The Porphyrin Handbook – Bioinorganic and Bioorganic Chemistry*, vol. 11. *The Porphyrin Handbook* (eds. K. M. Kadish, K. M. Smith & R. Guilard), pp. 51–73. San Diego, CA: Academic Press.
- GUNNER, M. R. & HONIG, B. (1991). Electrostatic control of midpoint potentials in the cytochrome subunit of the *Rhodospseudomonas viridis* reaction center. *Proceedings of the National Academy of Sciences USA* **88**, 9151–9155.
- GUNNER, M. R., NICHOLLS, A. & HONIG, B. (1996). Electrostatic potentials in *Rhodospseudomonas viridis* reaction centers: implications for the driving force and directionality of electron transfer. *Journal of Physical Chemistry* **100**, 4277–4291.
- GUNNER, M. R., ROBERTSON, D. E. & DUTTON, P. L. (1986). Kinetic studies on the reaction center protein from *Rhodospseudomonas sphaeroides* – the temperature and free-energy dependence of electron transfer between various quinones in the  $\text{Q}_A$  site and the oxidized bacteriochlorophyll dimer. *Journal of Physical Chemistry* **90**, 3783–3795.
- HARRIMAN, A. (1987). Further comments on the redox potentials of tryptophan and tyrosine. *Journal of Physical Chemistry* **91**, 6102–6104.
- HEITEL, H., MICHEL-BEYERLE, M. E. & FINCKH, P. (1987). Electron transfer through intramolecular bridges in donor/acceptor systems. *Chemical Physics Letters* **134**, 273–278.
- HERZ, T., OTTO, P. & CLARK, T. (2000). On the band gap in peptide  $\alpha$ -helices. *International Journal of Quantum Chemistry* **79**, 120–124.
- HOFBAUER, W., ZOUNI, A., BITTL, R., KERN, J., ORTH, P., LENDZIAN, F., FROMME, P., WITT, H. T. & LUBITZ, W. (2001). Photosystem II single crystals studied by EPR spectroscopy at 94 GHz: The tyrosine radical  $\text{Y}_D^\bullet$ . *Proceedings of the National Academy of Sciences USA* **98**, 6623–6628.
- HOFFMAN, B. M. & RATNER, M. A. (1987). Gated electron transfer: when are observed rates controlled by conformational interconversion? *Journal of the American Chemical Society* **109**, 6237–6243.

- HOPFIELD, J. J. (1974). Electron transfer between biological molecules by thermally activated tunneling. *Proceedings of the National Academy of Sciences USA* **71**, 3640–3644.
- IGUCHI, K. (1997). Semiconductivity of protein: the Saxon–Hutner–Luttinger Theorem in biopolymers. *International Journal of Modern Physics (B)* **11**, 2941–2960.
- IWATA, S., OSTERMEIER, C., LUDWIG, B. & MICHEL, H. (1995). Structure at 2.8 Å resolution of cytochrome *c* oxidase from *Paracoccus denitrificans*. *Nature* **376**, 660–669.
- JORTNER, J., BIXON, M., LANGENBACHER, T. L. & MICHEL-BEYERLE, M. E. (1998). Charge transfer and transport in DNA. *Proceedings of the National Academy of Sciences USA* **95**, 12759–12765.
- JOVANIC, S. V., HARRIMAN, A. & SIMIC, M. G. (1986). Electron-transfer reactions of tryptophan and tyrosine derivatives. *Journal of Physical Chemistry* **90**, 1935–1939.
- KARPISHIN, T. B., GRINSTAFF, M. W., KOMAR-PANICUCCI, S., MCLENDON, G. & GRAY, H. B. (1994). Electron transfer in cytochrome *c* depends upon the structure of the intervening medium. *Structure* **2**, 415–422.
- KIRMAIER, C. & HOLTEN, D. (1987). Primary photochemistry of reaction centers from the photosynthetic bacteria. *Photosynthesis Research* **13**, 225–260.
- KOMIYA, H., YEATES, T. O., REES, D. C., ALLEN, J. P. & FEHER, G. (1988). Structure of the reaction center from *Rhodobacter sphaeroides* R-26 and 2.41 – symmetry relations and sequence comparisons between different species. *Proceedings of the National Academy of Sciences USA* **85**, 9012–9016.
- KUULA, D., BAXTER, W. W., NATAN, M. J. & HOFFMAN, B. M. (1991). Temperature-independent electron transfer in mixed-metal hemoglobin hybrids. *Journal of Physical Chemistry* **95**, 1–3.
- KUKI, A. & WOLYNES, P. G. (1987). Electron tunneling paths in proteins. *Science* **236**, 1647–1652.
- KUMAR, K., KURNIKOV, I. V., BERATAN, D. N., WALDECK, D. H. & ZIMM, M. B. (1998). Use of modern electron transfer theories to determine the electronic coupling matrix elements in intramolecular systems. *Journal of Physical Chemistry (A)* **102**, 5529–5541.
- KUZNETSOV, A. M. & ULSTRUP, J. (1998). *Electron Transfer in Chemistry and Biology: An Introduction to the Theory*. Hoboken, NJ: John Wiley & Sons, Inc.
- LANGEN, R. (1995). Electron transfer in proteins: theory and experiment. Ph.D. thesis, California Institute of Technology.
- LANGEN, R., CHANG, I.-J., GERMANAS, J. P., RICHARDS, J. H., WINKLER, J. R. & GRAY, H. B. (1995). Electron tunneling in proteins: coupling through a  $\beta$ -strand. *Science* **268**, 1733–1735.
- LANGEN, R., COLÓN, J. L., CASIMIRO, D. R., KARPISHIN, T. B., WINKLER, J. R. & GRAY, H. B. (1996). Electron tunneling in proteins. Role of the intervening medium. *Journal of Biological Inorganic Chemistry* **1**, 221–225.
- LAWSON, J. M., CRAIG, D. C., PADDON-ROW, M. N., KROON, J. & VERHOEVEN, J. W. (1989). Through-bond modulation of intramolecular electron transfer in rigidly linked donor-acceptor systems. *Chemical Physics Letters* **164**, 120–125.
- LIANG, C. & NEWTON, M. D. (1992). Ab initio studies of electron transfer: pathway analysis of effective transfer integrals. *Journal of Physical Chemistry* **96**, 2855–2866.
- LIN, X., MURCHISON, H. A., NAGARAJAN, V., PARSON, W. W., ALLEN, J. P. & WILLIAMS, J. C. (1994a). Specific alteration of the oxidation potential of the electron donor in reaction centers from *Rhodobacter sphaeroides*. *Proceedings of the National Academy of Sciences USA* **91**, 10265–10269.
- LIN, X., WILLIAMS, J. C., ALLEN, J. P. & MATHIS, P. (1994b). Relationship between rate and free energy difference for electron transfer from cytochrome *c<sub>2</sub>* to the reaction center in *Rhodobacter sphaeroides*. *Biochemistry* **33**, 13517–13523.
- LO CONTE, L., CHOTHIA, C. & JANIN, J. (1999). The atomic structure of protein–protein recognition sites. *Journal of Molecular Biology* **285**, 2177–2198.
- MARCUS, R. A. (1956). On the theory of oxidation–reduction reactions involving electron transfer. I. *Journal of Chemical Physics* **24**, 966–978.
- MARCUS, R. A. & SUTIN, N. (1975). Electron-transfer reactions with unusual activation parameters. A treatment of reactions accompanied by large entropy decreases. *Inorganic Chemistry* **14**, 213–216.
- MARCUS, R. A. & SUTIN, N. (1985). Electron transfers in chemistry and biology. *Biochimica et Biophysica Acta* **811**, 265–322.
- MAUK, A. G., MAUK, M. R., MOORE, G. R. & NORTHRUP, S. H. (1995). Experimental and theoretical analysis of the interaction between cytochrome *c* and cytochrome *b<sub>5</sub>*. *Journal of Bioenergetics and Biomembranes* **27**, 311–330.
- MAUK, A. G., SCOTT, R. A. & GRAY, H. B. (1980). Distances of electron transfer to and from metalloprotein redox sites in reactions with inorganic complexes. *Journal of the American Chemical Society* **102**, 4360–4363.
- MAUK, M. R., REID, L. S. & MAUK, A. G. (1982). Spectrophotometric analysis of the interaction between cytochrome *b<sub>5</sub>* and cytochrome *c*. *Biochemistry* **21**, 1843–1846.
- MCCLESKEY, T. M., WINKLER, J. R. & GRAY, H. B. (1992). Driving-force effects on the rates of bimolecular electron-transfer reactions. *Journal of the American Chemical Society* **114**, 6935–6937.
- MCCONNELL, H. M. (1961). Intramolecular charge transfer in aromatic free radicals. *Journal of Chemical Physics* **35**, 508–515.
- MCGOURTY, J. L., BLOUGH, N. V. & HOFFMAN, B. M. (1983). Electron transfer at crystallographically known long distances (25-Å) in [Zn(II),Fe(III)] hybrid hemoglobin. *Journal of the American Chemical Society* **105**, 4470–4472.



- McLENDON, G. & HAKE, R. (1992). Interprotein electron transfer. *Chemical Reviews* **92**, 481–490.
- McLENDON, G. & MILLER, J. R. (1985). The dependence of biological electron-transfer rates on exothermicity: the cytochrome *c*/cytochrome *b<sub>5</sub>* couple. *Journal of the American Chemical Society* **107**, 7811–7816.
- McLENDON, G., ZHANG, Q., WALLIN, S. A., MILLER, R. M., BILLSTONE, V., SPEARS, K. G. & HOFFMAN, B. M. (1993). Thermodynamic and kinetic aspects of binding in the cytochrome *c*/cytochrome *c* peroxidase complex. *Journal of the American Chemical Society* **115**, 3665–3669.
- MEADE, T. J., GRAY, H. B. & WINKLER, J. R. (1989). Driving-force effects on the rate of long-range electron transfer in ruthenium-modified cytochrome *c*. *Journal of the American Chemical Society* **111**, 4353–4356.
- MEDVEDEV, D. M., DAIZADEH, I. & STUCHEBRUKHOV, A. A. (2000). Electron transfer tunneling pathways in bovine heart cytochrome *c* oxidase. *Journal of the American Chemical Society* **122**, 6571–6582.
- MEYER, T. E., RIVERA, M., WALKER, F. A., MAUK, M. R., MAUK, A. G., CUSANOVICH, M. A. & TOLLIN, G. (1993). Laser flash photolysis studies of electron transfer to the cytochrome *b<sub>5</sub>*-cytochrome *c* complex. *Biochemistry* **32**, 622–627.
- MILLER, J. R., BEITZ, J. V. & HUDDLESTON, R. K. (1984). Effect of free energy on rates of electron transfer between molecules. *Journal of the American Chemical Society* **106**, 5057–5068.
- MINES, G. A., BJERRUM, M. J., HILL, M. G., CASIMIRO, D. R., CHANG, I.-J., WINKLER, J. R. & GRAY, H. B. (1996). Rates of heme oxidation and reduction in Ru(His33)cytochrome *c* at very high driving forces. *Journal of the American Chemical Society* **118**, 1961–1965.
- MOORE, G. R. & PETTIGREW, G. W. (1990). *Cytochromes c: Evolutionary, Structural, and Physicochemical Aspects*. New York: Springer-Verlag.
- MOSER, C. C., KESKE, J. M., WARNCKE, K., FARID, R. S. & DUTTON, P. L. (1992). Nature of biological electron transfer. *Nature* **355**, 796–802.
- NEWTON, M. D. (1988). Electronic structure analysis of electron-transfer matrix elements for transition metal redox pairs. *Journal of Physical Chemistry* **92**, 3049–3056.
- NOCEK, J. M., ZHOU, J. S., DEFORD, S., PRIYADARSHY, S., BERATAN, D. N., ONUCHIC, J. N. & HOFFMAN, B. M. (1996). Theory and practice of electron transfer within protein-protein complexes: application to the multi-domain binding of cytochrome *c* by cytochrome *c* peroxidase. *Chemical Reviews* **96**, 2459–2489.
- ONUCHIC, J. N. & BERATAN, D. N. (1990). A predictive theoretical model for electron tunneling pathways in proteins. *Journal of Chemical Physics* **92**, 722–733.
- ONUCHIC, J. N., BERATAN, D. N., WINKLER, J. R. & GRAY, H. B. (1992). Pathway analysis of protein electron transfer reactions. *Annual Review of Biophysics and Biomolecular Structure* **21**, 349–377.
- ORTEGA, J. M. & MATHIS, P. (1993). Electron transfer from the tetraheme cytochrome to the special pair in isolated reaction centers of *Rhodospseudomonas viridis*. *Biochemistry* **32**, 1141–1151.
- OVERFIELD, R. E., SCHERZ, A., KAUFMANN, K. J. & WASIELEWSKI, M. R. (1983). Photoinduced electron-transfer reactions in a chlorophyllide-pheophorbide cyclophane. A model for photosynthetic reaction centers. *Journal of the American Chemical Society* **105**, 5747–5752.
- PADDON-ROW, M. N. (2003). Superexchange-mediated charge separation and charge recombination in covalently linked donor-bridge-acceptor systems. *Australian Journal of Chemistry* **56**, 729–748.
- PAGE, C. C., MOSER, C. C., CHEN, X. & DUTTON, P. L. (1999). Natural engineering principles of electron tunnelling in biological oxidation-reduction. *Nature* **402**, 47–52.
- PAN, L. P., HIBDON, S., LIU, R.-Q., DURHAM, B. & MILLETT, F. (1993). Intracomplex electron transfer between ruthenium-cytochrome *c* derivatives and cytochrome *c* oxidase. *Biochemistry* **32**, 8492–8498.
- PASCHER, T., CHESICK, J. P., WINKLER, J. R. & GRAY, H. B. (1996). Protein folding triggered by electron transfer. *Science* **271**, 1558–1560.
- PASCHER, T., KARLSSON, B. G., NORDLING, M., MALMSTRÖM, B. G. & VANNGARD, T. (1993). Reduction potentials and their pH dependence in site-directed mutant forms of azurin from *Pseudomonas aeruginosa*. *European Journal of Biochemistry* **212**, 289–296.
- PASMAN, P., KOPER, N. W. & VERHOEVEN, J. W. (1982). Photoinduced long-range electron transfer in rigid bichromophoric molecules. *Recueil des Travaux Chimiques des Pays-Bas [Journal of the Royal Netherlands Chemical Society]* **101**, 363–364.
- PELLETIER, H. & KRAUT, J. (1992). Crystal structure of a complex between electron-transfer partners, cytochrome *c* peroxidase and cytochrome *c*. *Science* **258**, 1748–1755.
- PETERSON-KENNEDY, S. E., MCGOURTY, J. L., KALWEIT, J. A. & HOFFMAN, B. M. (1986). Temperature dependence of and ligation effects on long-range electron transfer in complementary [Zn,Fe<sup>III</sup>]hemoglobin hybrids. *Journal of the American Chemical Society* **108**, 1739–1746.
- PLETNEVA, E. V., FULTON, D. B., KOHZUMA, T. & KOSTIC, N. M. (2000). Protein docking and gated electron-transfer reactions between zinc cytochrome *c* and the new plastocyanin from the fern *Dryopteris crassiribizoma*. Direct kinetic evidence for multiple binary complexes. *Journal of the American Chemical Society* **122**, 1034–1046.
- PONCE, A., GRAY, H. B. & WINKLER, J. R. (2000). Electron tunneling through water: oxidative quenching of electronically excited Ru(tpy)<sub>2</sub><sup>2+</sup> (tpy = 2,2':6,2''-terpyridine) by ferric ion in aqueous glasses at 77 K. *Journal of the American Chemical Society* **122**, 8187–8191.

- POULOS, T. L. & KRAUT, J. (1980). A hypothetical model of the cytochrome *c* peroxidase • cytochrome *c* electron transfer complex. *Journal of Biological Chemistry* **255**, 10322–10330.
- QIN, L., RODGERS, K. K. & SLIGAR, S. G. (1991). Electron transfer between cytochrome *b<sub>5</sub>* surface mutants and cytochrome *c*. *Molecular Crystals and Liquid Crystals* **194**, 311–316.
- RAMIREZ, B. E., MALMSTRÖM, B. G., WINKLER, J. R. & GRAY, H. B. (1995). The currents of life: the terminal electron-transfer complex of respiration. *Proceedings of the National Academy of Sciences USA* **92**, 11949–11951.
- REGAN, J. J., DI BILIO, A. J., LANGEN, R., SKOV, L. K., WINKLER, J. R., GRAY, H. B. & ONUCHIC, J. N. (1995). Electron tunneling in azurin: coupling across a  $\beta$  sheet. *Chemistry and Biology* **2**, 489–496.
- REGAN, J. J. & ONUCHIC, J. N. (1999). Electron-transfer tubes. *Advances in Chemical Physics* **107**, 497–553.
- REGAN, J. J., RAMIREZ, B. E., WINKLER, J. R., GRAY, H. B. & MALMSTRÖM, B. G. (1998). Pathways for electron tunneling in cytochrome *c* oxidase. *Journal of Bioenergetics and Biomembranes* **30**, 35–39.
- REHM, D. & WELLER, A. (1970). Kinetics of fluorescence quenching by electron and H-atom transfer. *Israel Journal of Chemistry* **8**, 259–271.
- ROBERTS, V. A. & PIQUE, M. E. (1999). Definition of the interaction domain for cytochrome *c* on cytochrome *c* oxidase. III. Prediction of the docked complex by a complete systematic search. *Journal of Biological Chemistry* **274**, 38051–38060.
- SABAHI, A. & WITTUNG-STAFSHED, P. (2002). Unfolding the unique  $\alpha$ -type heme protein, *Chlamydomonas reinhardtii* cytochrome *f*. *Biochimica et Biophysica Acta – Protein Structure and Molecular Enzymology* **1596**, 163–171.
- SALEMME, F. R. (1976). Hypothetical structure for an intermolecular electron transfer complex of cytochrome *c* and cytochrome *b<sub>5</sub>*. *Journal of Molecular Biology* **102**, 563–568.
- SCOTT, R. A. & MAUK, A. G. (1996). *Cytochrome *c* – A Multidisciplinary Approach*, pp. 738. Sausalito, CA: University Science Books.
- SHEU, S.-Y., YANG, D.-Y., SELZLE, H. L. & SCHLAG, E. W. (2002). Charge transport in a polypeptide chain. *European Physical Journal (D)* **20**, 557–563.
- SHOPES, R. J., LEVINE, L. M. A., HOLTEN, D. & WRAIGHT, C. A. (1987). Kinetics of oxidation of the bound cytochromes in reaction centers from *Rhodospseudomonas viridis*. *Photosynthesis Research* **12**, 165–180.
- SIMOLO, K. P., MCLENDON, G. L., MAUK, M. R. & MAUK, A. G. (1984). Photoinduced electron transfer within a protein-protein complex formed between physiological redox partners – reduction of ferricytochrome *b<sub>5</sub>* by the hemoglobin derivative  $\alpha_2\text{Zn-}\beta_2\text{Fe}^{\text{III}}(\text{CN})$ . *Journal of the American Chemical Society* **106**, 5012–5013.
- SIMONSON, T. (2002). Gaussian fluctuations and linear response in an electron transfer protein. *Proceedings of the National Academy of Sciences USA* **99**, 6544–6549.
- SKOURTIS, S. S. & BERATAN, D. N. (1997). High and low resolution theories of protein electron transfer. *Journal of Biological Inorganic Chemistry* **2**, 378–386.
- SKOURTIS, S. S. & BERATAN, D. N. (1998). Electron transfer mechanisms. *Current Opinion in Chemical Biology* **2**, 235–243.
- SKOV, L. K., PASCHER, T., WINKLER, J. R. & GRAY, H. B. (1998). Rates of intramolecular electron transfer in  $\text{Ru}(\text{bpy})_2(\text{im})(\text{His83})$ -modified azurin increase below 220 K. *Journal of the American Chemical Society* **120**, 1102–1103.
- SMALLEY, J. F., FELDBERG, S. W., CHIDSEY, C. E. D., LINFORD, M. R., NEWTON, M. D. & LIU, Y.-P. (1995). The kinetics of electron transfer through ferrocene-terminated alkanethiol monolayers on gold. *Journal of Physical Chemistry* **99**, 13141–13149.
- SMALLEY, J. F., FINKLEA, H. O., CHIDSEY, C. E. D., LINFORD, M. R., CREAGER, S. E., FERRARIS, J. P., CHALFANT, K., ZAWODZINSKI, T., FELDBERG, S. W. & NEWTON, M. D. (2003). Heterogeneous electron-transfer kinetics for ruthenium and ferrocene redox moieties through alkanethiol monolayers on gold. *Journal of the American Chemical Society* **125**, 2004–2013.
- SPRINGS, S. L., BASS, S. E., BOWMAN, G., NODELMAN, I., SCHUTT, C. E. & MCLENDON, G. L. (2002). A multi-generation analysis of cytochrome *b<sub>562</sub>* redox variants: strategies for modulating redox potential revealed using a library approach. *Biochemistry* **41**, 4321–4328.
- STEMP, E. D. A. & HOFFMAN, B. M. (1993). Cytochrome *c* peroxidase binds two molecules of cytochrome *c*: evidence for a low-affinity, electron-transfer-active site on cytochrome *c* peroxidase. *Biochemistry* **32**, 10848–10865.
- STUBBE, J., NOCERA, D. G., YEE, C. S. & CHANG, M. C. Y. (2003). Radical initiation in the class I ribonucleotide reductase: long-range proton-coupled electron transfer? *Chemical Reviews* **103**, 2167–2201.
- STUBBE, J. & VAN DER DONK, W. A. (1998). Protein radicals in enzyme catalysis. *Chemical Reviews* **98**, 705–762.
- STUCHEBRUKHOV, A. A. (1996). Tunneling currents in electron-transfer reactions in proteins. 2. Calculation of electronic superexchange matrix element and tunneling currents using nonorthogonal basis sets. *Journal of Chemical Physics* **105**, 10819–10829.
- STUCHEBRUKHOV, A. A. (2001). Toward *ab initio* theory of long-distance electron tunneling in proteins: tunneling currents approach. *Advances in Chemical Physics* **118**, 1–44.
- SUCHETA, A., SZUNDI, I. & EINARSDOTTIR, O. (1998). Intermediates in the reaction of fully reduced cytochrome *c* oxidase with dioxygen. *Biochemistry* **37**, 17905–17914.
- SZENT-GYÖRGYI, A. (1941). Towards a new biochemistry? *Science* **93**, 609–611.

- TEZCAN, F. A., CRANE, B. R., WINKLER, J. R. & GRAY, H. B. (2001). Electron tunneling in protein crystals. *Proceedings of the National Academy of Sciences USA* **98**, 5002–5006.
- TEZCAN, F. A., WINKLER, J. R. & GRAY, H. B. (1998). Effects of ligation and folding on reduction potentials of heme proteins. *Journal of the American Chemical Society* **120**, 13383–13388.
- TOMMOS, C., SKALICKY, J. J., PILOUD, D. L., WAND, A. J. & DUTTON, P. L. (1999). De novo proteins as models of radical enzymes. *Biochemistry* **38**, 9495–9507.
- TSUKIHARA, T., AOYAMA, H., YAMASHITA, E., TOMIZAKI, T., YAMAGUCHI, H., SHINZAWA-ITOH, K., NAKASHIMA, R., YAONO, R. & YOSHIKAWA, S. (1995). Structures of metal sites of oxidized bovine heart cytochrome *c* oxidase at 2.8 Å. *Science* **269**, 1071–1074.
- VARADARAJAN, R., ZEWEIT, T. E., GRAY, H. B. & BOXER, S. G. (1989). Effects of buried ionizable amino acids on the reduction potential of recombinant myoglobin. *Science* **243**, 69–72.
- VENTUROLI, G., DREPPER, F., WILLIAMS, J. C., ALLEN, J. P., LIN, X. & MATHIS, P. (1998). Effects of temperature and  $\Delta G^\circ$  on electron transfer from cytochrome *c*<sub>2</sub> to the photosynthetic reaction center of the purple bacterium from *Rhodospirillum rubrum*. *Biophysical Journal* **74**, 3226–3240.
- VERHOEVEN, J. W. (1999). From close contact to long-range intramolecular electron transfer. *Advances in Chemical Physics* **106**, 603–644.
- WASIELEWSKI, M. R. (1992). Photoinduced electron transfer in supramolecular systems for artificial photosynthesis. *Chemical Reviews* **92**, 435–461.
- WILLIAMS, K. R., GAMELIN, D. R., LACROIX, L. B., HOUSER, R. P., TOLMAN, W. B., MULDER, T. C., DE VRIES, S., HEDMAN, B., HOSGSON, K. O. & SOLOMON, E. I. (1997). Influence of copper-sulfur covalency and copper-copper bonding on valence delocalization and electron transfer in the Cu<sub>A</sub> site of cytochrome *c* oxidase. *Journal of the American Chemical Society* **119**, 613–614.
- WINKLER, J. R. (2000). Electron tunneling pathways in proteins. *Current Opinion in Chemical Biology* **4**, 192–198.
- WINKLER, J. R., DI BILIO, A., FARROW, N. A., RICHARDS, J. H. & GRAY, H. B. (1999). Electron tunneling in biological molecules. *Pure and Applied Chemistry* **71**, 1753–1764.
- WINKLER, J. R. & GRAY, H. B. (1992). Electron transfer in ruthenium-modified proteins. *Chemical Reviews* **92**, 369–379.
- WINKLER, J. R., NOCERA, D. G., YOCOM, K. M., BORDIGNON, E. & GRAY, H. B. (1982). Electron-transfer kinetics of pentaammineruthenium(III)(histidine-33)-ferricytochrome *c*. Measurement of the rate of intramolecular electron transfer between redox centers separated by 15 Å in a protein. *Journal of the American Chemical Society* **104**, 5798–5800.
- WINKLER, J. R., WITTUNG-STAFSHED, P., LECKNER, J., MALMSTRÖM, B. G. & GRAY, H. B. (1997). Effects of folding on metalloprotein active sites. *Proceedings of the National Academy of Sciences USA* **94**, 4246–4249.
- WUTTKE, D. S., BJERRUM, M. J., WINKLER, J. R. & GRAY, H. B. (1992). Electron-tunneling pathways in cytochrome *c*. *Science* **256**, 1007–1009.
- YE, Y.-J. & LADIK, J. (1994). Theory of hopping conductivity of proteins. *International Journal of Quantum Chemistry* **52**, 491–506.
- YOCOM, K. M., SHELTON, J. B., SHELTON, J. R., SCHROEDER, W. E., WOROSILA, G., ISIED, S. S., BORDIGNON, E. & GRAY, H. B. (1982). Preparation and characterization of a pentammineruthenium(III) derivative of horse heart ferricytochrome *c*. *Proceedings of the National Academy of Sciences USA* **79**, 7052–7055.
- YOSHIKAWA, S., SHINZAWA-ITOH, K., NAKASHIMA, R., YAONO, R., YAMASHITA, E., INOUE, N., YAO, M., FEI, J. M., LIBEU, C. P., MIZUSHIMA, T., YAMAGUCHI, H., TOMIZAKI, T. & TSUKIHARA, T. (1998). Redox-coupled crystal structural changes in bovine heart cytochrome *c* oxidase. *Science* **280**, 1723–1729.